JACALIN-LECTIN LIKE1 Regulates the Nuclear Accumulation of GLYCINE-RICH RNA-BINDING PROTEIN7, Influencing the RNA Processing of *FLOWERING LOCUS C* Antisense Transcripts and Flowering Time in Arabidopsis[1][OPEN]

Jun Xiao[2,3], Chunhua Li[2], Shujuan Xu, Lijing Xing, Yunyuan Xu, and Kang Chong*

Key Laboratory of Plant Molecular Physiology, Institute of Botany, Chinese Academy of Sciences, Beijing 100093, China (J.X., C.L., S.X., L.X., Y.X., K.C.); National Center for Plant Gene Research, Beijing 100093, China (K.C.); and University of the Chinese Academy of Sciences, Beijing 100049, China (J.X., C.L., S.X.)

ORCID ID: 0000-0003-1687-9833 (S.X.).

Lectins selectively recognize sugars or glycans for defense in living cells, but less is known about their roles in the development process and the functional network with other factors. Here, we show that Arabidopsis (*Arabidopsis thaliana*) JACALIN-LECTIN LIKE1 (AtJAC1) functions in flowering time control. Loss of function of AtJAC1 leads to precocious flowering, whereas overexpression of AtJAC1 causes delayed flowering. AtJAC1 influences flowering through regulation of the key flowering repressor gene *FLOWERING LOCUS C* (*FLC*). Genetic analysis revealed that AtJAC1's function is mostly dependent on GLYCINE-RICH RNA-BINDING PROTEIN7 (GRP7), an upstream regulator of *FLC*. Biochemical and cell biological data indicated that AtJAC1 interacted physically with GRP7 specifically in the cytoplasm. AtJAC1 influences the nucleocytoplasmic distribution of GRP7, with predominant nuclear localization of GRP7 when AtJAC1 function is lost but retention of GRP7 in the cytoplasm when AtJAC1 is overexpressed. A temporal inducible assay suggested that AtJAC1's regulation of flowering could be compromised by the nuclear accumulation of GRP7. In addition, GRP7 binds to the antisense precursor messenger RNA of *FLC* through a conserved RNA motif. Loss of GRP7 function leads to the elevation of total *FLC* antisense transcripts and reduced proximal-distal polyadenylation ratio, as well as histone methylation changes in the *FLC* gene body region and increased total functional sense *FLC* transcript. Attenuating the direct binding of GRP7 with competing artificial RNAs leads to changes of *FLC* antisense precursor messenger RNA processing and flowering transition. Taken together, our study indicates that AtJAC1 coordinates with GRP7 in shaping plant development through the regulation of RNA processing in Arabidopsis.

Lectins are highly diverse proteins that selectively recognize specific free sugars or glycans present on glycoproteins and glycolipids (Peumans and Van Damme, 1995). They are widespread among living organisms and are involved in diverse biological processes (Moreira et al., 1991; Sharon, 2008). In animals, they are involved in self-recognition and cell-to-cell interaction in addition to acting as chaperones during glycoprotein synthesis (Rabinovich and Toscano, 2009; Lam and Ng, 2011). In plants, they serve as storage proteins and have roles in defense against pathogens and insect pests (Peumans and Van Damme, 1995; Babosha, 2008; Vandenborre et al., 2011). As a subgroup of lectins, Jacalin-lectin proteins have one or more jacalin-like lectin domains with binding specificity to Man or Gal (Kabir, 1998; Peumans et al., 2001). They are involved in multiple biological processes (Aucouturier et al., 1989; Yong et al., 2003; Jiang et al., 2006). Arabidopsis (*Arabidopsis thaliana*) JASMONATE ACID RESPONSE1 and wheat (*Triticum aestivum*) JACALIN-RELATED LECTIN LIKE1 are involved in jasmonic acid-mediated defense responses (León et al., 1998; Xiang et al., 2011). In rice (*Oryza sativa*), JACALIN-RELATED LECTIN1 (OsJAC1) suppresses the coleoptiles and stem elongation (Jiang et al., 2006). In wheat, a jacalin-like lectin, VER2, is induced during vernalization in young leaves and the shoot apical meristem, thus regulating flowering and spikelet development (Chong et al., 1998; Yong et al.,

[1] This work was supported by the major state basic research program of China (973 Program; grant no. 2011CB915404) and the China-Netherlands Joint Scientific Thematic Research Program (grant no. GJHZ1309).

[2] These authors contributed equally to the article.

[3] Present address: Department of Biology, University of Pennsylvania, 433 S. University Avenue, Philadelphia, PA 19104.

* Address correspondence to chongk@ibcas.ac.cn.

The author responsible for distribution of materials integral to the findings presented in this article in accordance with the policy described in the Instructions for Authors (www.plantphysiol.org) is: Kang Chong (chongk@ibcas.ac.cn).

J.X. and K.C. designed the project; J.X., C.L., and S.X. performed the experiments; J.X., C.L., L.X., Y.X., and K.C. analyzed and interpreted the data; J.X. and K.C. wrote the article; all authors approved the article.

[OPEN] Articles can be viewed without a subscription.

www.plantphysiol.org/cgi/doi/10.1104/pp.15.00801

2003). Recently, we found that this is mainly mediated by the interaction between VER2 and proteins with *O*-GlcNAc modification during the course of vernalization (Xing et al., 2009; Xiao et al., 2014). To date, whether Jacalin-lectin functions in development regulation and how it cooperates with other factors are still unclear in dicotyledons such as Arabidopsis.

Flowering is an important developmental transition during the life cycle of plants. It is precisely regulated by endogenous programs and environmental cues (Fornara et al., 2010). In Arabidopsis, flowering is regulated by five major pathways: vernalization, photoperiod, GA, autonomous, and age (Amasino, 2010; Srikanth and Schmid, 2011; Song et al., 2013a; Romera-Branchat et al., 2014). Multiple genetic pathways converge to regulate the expression of *FLOWERING LOCUS C* (*FLC*), which encodes a MADS box transcription factor that plays a key role in the repression of flowering (Michaels and Amasino, 1999; Sheldon et al., 1999). During long-term cold, the vernalization pathway epigenetically silences *FLC* (Song et al., 2013a). In ambient temperatures, the FRIGIDA pathway up-regulates *FLC* expression while the autonomous pathway down-regulates *FLC* (Amasino, 2010; Crevillén and Dean, 2011). Chromatin modification and RNA processing are involved in the precise regulation of *FLC* transcription under both cold (vernalization) and ambient temperatures (He, 2012; Song et al., 2013a; Csorba et al., 2014). Autonomous pathway members, the RNA-binding proteins FCA and FPA, together with the 3′ processing factors CLEAVAGE STIMULATING FACTOR64 (CstF64), CstF77, and FY are involved in the polyadenylation site selection of a set of antisense transcripts of *FLC*, named *COOLAIR* (Swiezewski et al., 2009; Hornyik et al., 2010; Liu et al., 2010). The alternative usage of polyadenylation sites of *COOLAIR* is coupled with the expression state of a functional *FLC* sense transcript in a process requiring the histone H3K4me2 demethylase FLOWERING LOCUS D (Liu et al., 2007) and the positive transcription elongation factor b complex component CYCLIN-DEPENDENT KINASE C (Wang et al., 2014).

A member of the highly conserved small Gly-rich RNA-binding proteins (GRPs; Mangeon et al., 2010), GRP7, is also reported to regulate flowering in the autonomous pathway (Streitner et al., 2008). It contains an N-terminal RNA recognition motif and a C-terminal Gly-rich domain with nucleocytoplasmic shuttling ability (Lummer et al., 2011). GRP7 has multiple functions in RNA processing, including RNA chaperone activity (Kim et al., 2007), facilitating messenger RNA (mRNA) transport from the nucleus to the cytoplasm (Kim et al., 2008), regulating precursor messenger RNA (premRNA) splicing (Streitner et al., 2012), and processing of the primary microRNA (Köster et al., 2014). However, how GRP7 is involved in the regulation of flowering and the direct target of GRP7 in the flowering control network are unknown.

Here, we report that the Jacalin-lectin AtJAC1 functions in flowering time control in Arabidopsis. AtJAC1 interacts genetically and physically with GRP7 to regulate the *FLC* functional transcript level, which is coupled by influencing the RNA processing of *COOLAIR* through direct binding of GRP7 to *FLC* antisense premRNA.

RESULTS

Jacalin-Lectin AtJAC1 Regulates Flowering Time in Arabidopsis

Phylogenetic analysis based on the amino acid sequence similarity of the Jacalin domain showed that there were 15 proteins in Arabidopsis that are potential orthologs of wheat Jacalin-lectin VER2 (Supplemental Fig. S1A), which is induced by cold and regulates vernalization-mediated flowering in wheat (Yong et al., 2003; Xiao et al., 2014). Among those genes, AtJAC1 (At3g16470) contained three Jacalin-lectin domains with hemagglutination activity and could bind Man, Rib, and Glc with high affinity (Supplemental Fig. S1, B–E; Supplemental Table S1). AtJAC1 is expressed in lots of tissues, with a dynamic expression level in the shoot apex during the floral transition process (Supplemental Fig. S1F), indicating its potential role in flowering time regulation.

To investigate whether AtJAC1 plays a role in the floral transition, two transfer DNA (T-DNA) insertion mutants of *AtJAC1* were obtained from SALK (Alonso et al., 2003). In the null mutant *atjac1-1* (*SALK_000461*), T-DNA was inserted in the first exon to cause the absence of the full-length mRNA of *AtJAC1*, whereas in *atjac1-2* (*SALK_112556*), T-DNA was inserted into the intergenic region between *At3g16470* (*AtJAC1*) and *At3g16460*, causing the down-regulation of both genes (Fig. 1A; Supplemental Fig. S2A). At3g16460 (AtJAC2) was also predicted to be a jacalin-like lectin, with four jacalin-lectin domains (Supplemental Fig. S2B). However, its expression was low in the shoot apex (Supplemental Fig. S2C). A knockdown mutant of *At3g16460* (*atjac2*; *SALK_028332*) showed no change in flowering time compared with wild-type Columbia (Col; Supplemental Fig. S2, D and E). Contrarily, both *atjac1-1* and *atjac1-2* were early flowering, with significantly fewer rosette leaves when bolting compared with wild-type Col, under either long-day (LD) or short-day (SD) conditions (Fig. 1, B and C). Either vernalization or GA_3 treatment could accelerate the flowering of both *atjac1* mutants and Col, but still *atjac1* mutants flower slightly earlier than Col (Fig. 1, B and C). This suggests that AtJAC1 may not function in the vernalization- or GA-regulated flowering time pathways. Meanwhile, *AtJAC1* overexpression lines (*AtJAC1*-OE; Supplemental Fig. S2F) showed delayed flowering either under varied photoperiod conditions or with GA_3 treatment as compared with the control, ecotype C24, transformed with the empty vector *pBI121-GFP* (Fig. 1C). By contrast, vernalization rescued the delayed flowering of *AtJAC1*-OE lines to the control level (Fig. 1C). Furthermore, we performed

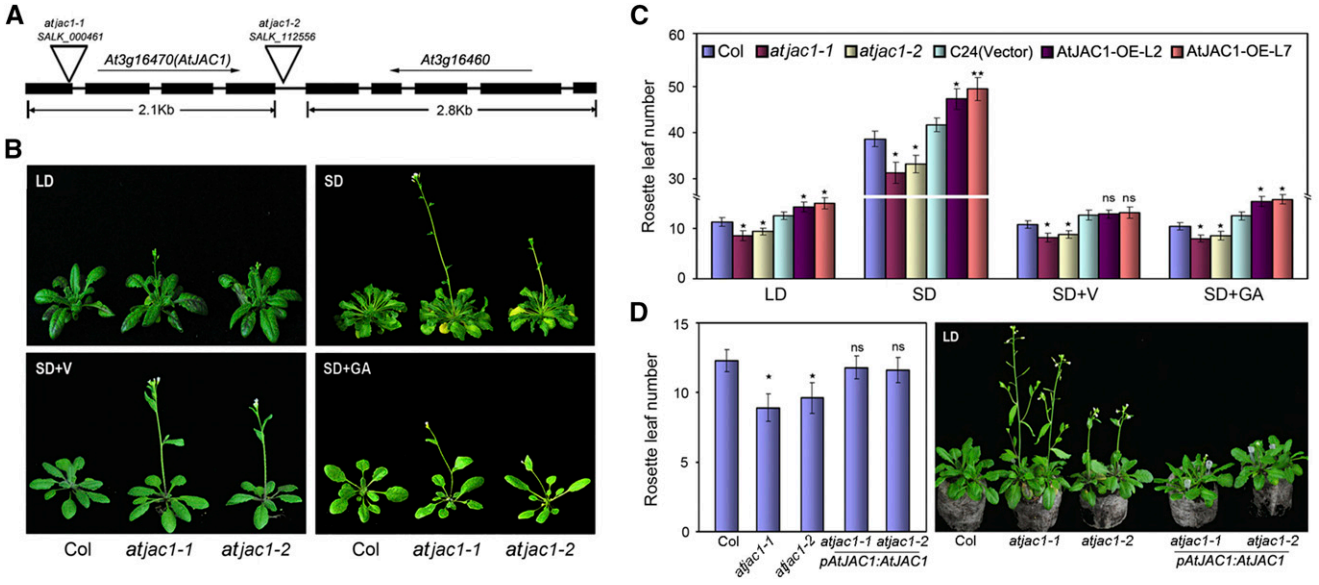

Figure 1. AtJAC1 inhibits the flowering transition in Arabidopsis. A, Schematic diagram of the T-DNA insertion sites of *atjac1-1* and *atjac1-2* mutants. B, *atjac1* mutants flowered earlier than the wild type (Col) under SD and LD conditions, SD conditions with vernalization (SD+V), and SD conditions with GA (SD+GA). C, Rosette leaf number at bolting in *atjac1* mutants, *AtJAC1*-OE plants, and controls (Col and C24 transformed with vector *pBI121-GFP*). D, Morphological phenotype and rosette leaf numbers in *atjac1-1*, *atjac1-2*, and genetic complementation lines with *pAtJAC1*::*AtJAC1*. Data are means ± SD of 15 plants for each line. Statistical analysis was done by Student's *t* test in C and D; *atjac1* mutants were compared with Col, whereas *AtJAC1*-OE lines were compared with C24 (vector). *, $P < 0.05$; **, $P < 0.01$; ns, no significant change.

genetic complementation by introducing *pAtJAC1*::*AtJAC1* in *atjac1-1* or *atjac1-2* mutants to confirm the function of AtJAC1 in flowering regulation (Fig. 1D; Supplemental Fig. S2G). As expected, the complementation lines rescued the early-flowering phenotype of both *atjac1-1* and *atjac1-2* (Fig. 1D). Taken together, *AtJAC1* negatively regulates flowering in Arabidopsis.

AtJAC1 Influences Flowering through the Regulation of *FLC* Transcript Level

AtJAC1 mutants and ectopic overexpression transgenic lines retain the photoperiodic response, which is even more severe in SD conditions (Fig. 1C), which is a feature of autonomous pathway regulators (He and Amasino, 2005). In addition, vernalization fully overcomes the late-flowering phenotype of *AtJAC1* overexpression lines (Fig. 1C), which is similar to the autonomous pathway late-flowering mutants (Bäurle and Dean, 2006). This hints at the possibility that AtJAC1 regulates flowering through the autonomous pathway. FLC is a key flowering repressor, integrating the inputs from autonomous pathway members (He, 2012). How the *FLC* response works in the floral repression effect of *AtJAC1* is an attractive issue.

To address this question, we quantified *FLC* mRNA expression in *AtJAC1* mutants and ectopic overexpression transgenic lines. The *FLC* mRNA level was reduced in *atjac1-1* and *atjac1-2* mutants but elevated in *AtJAC1*-OE lines (Fig. 2A). Concomitantly, *SUPRESSOR OF OVEREXPRESSION OF CONSTANS1* (*SOC1*) and *FLOWERING LOCUS T* (*FT*), which are negatively controlled by direct binding of *FLC*, were up-regulated in *atjac1* mutants but down-regulated in *AtJAC1*-OE lines (Fig. 2A). This suggests that *AtJAC1* may influence flowering time through the regulation of *FLC* expression. In addition, the *FLC* homologs *MADS AFFCTING FLOWERING1* (*MAF1*) and *MAF5*, but not *MAF2*, *MAF3*, and *MAF4*, showed a similar expression pattern to *FLC* in *atjac1* mutants and *AtJAC1-OE* lines, although the fold change is moderate (Fig. 2A). In contrast, the mRNA levels of other flowering pathway key regulators, such as *CONSTANS* (*CO*) of the photoperiod pathway (Putterill et al., 1995) and *SQUAMOSA PROMOTER BINDING PROTEIN-LIKE* (*SPL*) of the age pathway (Wang et al., 2009; Wu et al., 2009), were not significantly changed in either *atjac1* mutants or *AtJAC1*-OE lines (Supplemental Fig. S3).

To study the genetic relation between *FLC* and *AtJAC1*, the late-flowering lines *AtJAC1*-OE-L2 and *AtJAC1*-OE-L7 were crossed to a null mutant, *flc-20*, which has a Dissociation element insertion, leading to extremely early flowering (Helliwell et al., 2002). The F2 generation, homozygous for both the *flc-20* allele and *AtJAC1*-OE constructs, flowered almost the same time as *flc-20* plants in terms of rosette leaf number when bolting (Fig. 2B) but significantly earlier than the control (ecotype C24 transformed with the empty vector). Therefore, *AtJAC1* function genetically depends on *FLC* in the regulation of flowering.

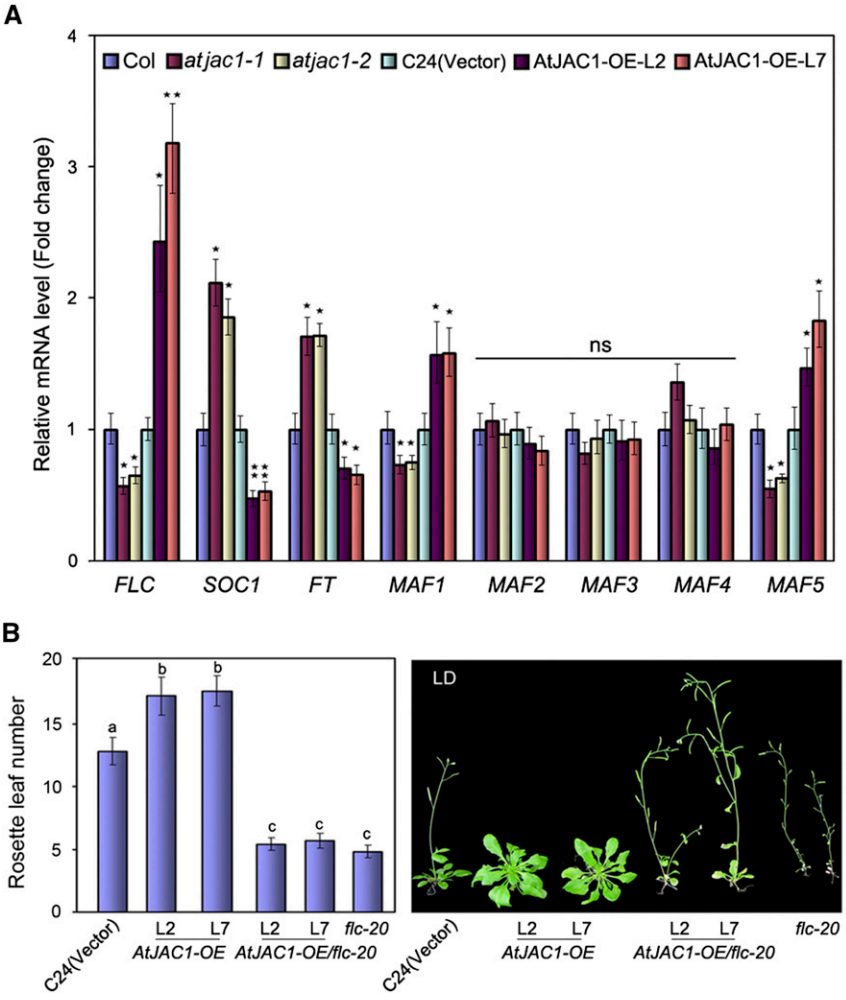

Figure 2. AtJAC1 influences flowering through the regulation of *FLC* transcript level. A, Transcript levels of key flowering genes in *atjac1* mutants and *AtJAC1*-OE plants (normalized to *Ubiquitin C* [*UBC*], a reference gene for quantitative PCR [qPCR]). Data are means ± SD of three parallel samples from one replicate, and three biological repeats were performed. B, Morphological phenotypes and rosette leaf numbers in *AtJAC1*-OE/*flc-20* under LD conditions. Statistical analysis was done by Student's *t* test in A; *atjac1* mutants were compared with Col, whereas *AtJAC1*-OE lines were compared with C24 (vector). *, $P < 0.05$; **, $P < 0.01$; ns, no significant change. Tukey's honestly significant difference (HSD) test was used for B, and different letters indicate statistically significant differences.

AtJAC1 Interacts Physically with GRP7 for the Regulation of *FLC* Transcript Level and Flowering

We previously reported that TaGRP2, an ortholog of the autonomous pathway member GRP7 in Arabidopsis, could interact physically with Jacalin-lectin VER2 in the regulation of flowering transition in wheat (Xiao et al., 2014). This may be a clue that AtJAC1 regulates *FLC* transcript level by directly interacting with GRP7.

To confirm this hypothesis, a coimmunoprecipitation (CoIP) assay was performed. FLAG-AtJAC1 was coexpressed with GRP7-GFP or GFP in tobacco (*Nicotiana tabacum*) leaves. After immunoprecipitation (IP) with GFP antibody, FLAG-AtJAC1 was detected in the elution of the FLAG-AtJAC1/GRP7-GFP coexpression line but not in that of the FLAG-AtJAC1/GFP line, demonstrating that AtJAC1 and GRP7 interacted in vivo (Fig. 3A). Bimolecular fluorescence complementation (BiFC) assays revealed that yellow fluorescent protein (YFP) signal generated from the interaction of AtJAC1 and GRP7 was only in the cytoplasm in Arabidopsis protoplasts (Fig. 3B). However, both AtJAC1-GFP and GRP7-GFP could localize in the cytoplasm and the nucleus (Supplemental Fig. S4A). Immunoblotting of nuclear and cytoplasmic fractions indicated that AtJAC1 and GRP7 were detected in both fractions (Fig. 3C; Supplemental Fig. S4, B and C). However, the IP assay showed that GRP7 was coimmunoprecipitated with AtJAC1 only in the cytoplasmic fraction and not the nuclear fraction (Fig. 3C). This further supports the idea that AtJAC1 and GRP7 directly interact specifically in the cytoplasm.

To further analyze their genetic relation, we generated the double mutant *atjac1-1 grp7-1* (Supplemental Fig. S5). The flowering time in each genotype was quantified by measuring the rosette leaf number when bolting. As reported previously (Streitner et al., 2008), the *grp7-1* single mutant is late flowering with more rosette leaves when bolting compared with Col (Fig. 3, D and E). In the F2 generation, the homozygous double mutant *atjac1-1 grp7-1* showed delayed flowering compared with Col and *atjac1-1* but similar to *grp7-1* (Fig. 3, D and E). As well, the *FLC* expression level coincides with the flowering time of different genotypes (Fig. 3E). Thus, AtJAC1 is genetically dependent on GRP7 in the regulation of *FLC* transcript level and flowering.

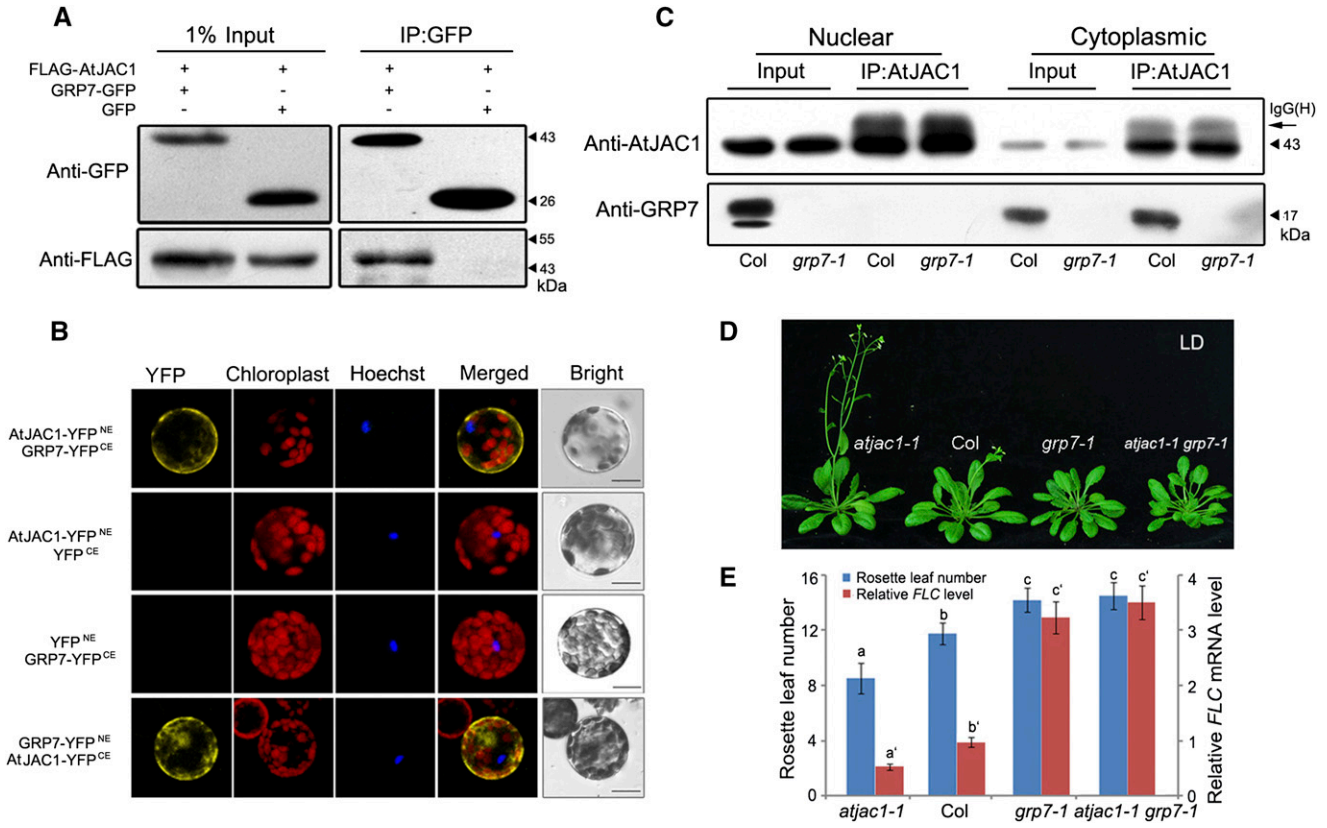

Figure 3. AtJAC1 interacts physically and genetically with GRP7 in the regulation of flowering. A, CoIP assay confirming the interaction between AtJAC1 and GRP7 in vivo. AtJAC1-FLAG together with GRP7-GFP or GFP were cotransfected into tobacco leaves, IP was performed with anti-GFP antibody, and immunoblotting was done with anti-FLAG antibody. B, BiFC assay showing the interaction between AtJAC1 and GRP7 in the cytoplasm in Arabidopsis protoplasts. Hoechst staining of nuclei is shown. Bars = 10 μm. C, CoIP assay of the interaction between AtJAC1 and GRP7 in the cytoplasm. Nuclear and cytoplasmic protein fractions were isolated from Col and *grp7-1* plants separately. IP was performed with anti-AtJAC1 antibody, and immunoblotting was done with anti-GRP7 antibody. IgG(H), IgG H chain. D and E, AtJAC1 regulates flowering through GRP7. Morphological phenotypes (D) as well as rosette leaf numbers and *FLC* mRNA levels (E) are shown in Col, *atjac1-1*, *grp7-1*, and *atjac1-1 grp7-1* double mutants. Tukey's HSD test was performed for E. Letters with or without ′ represent different groups; different letters indicate statistically significant differences within groups.

AtJAC1 Inhibits the Nuclear Accumulation of GRP7

The opposite phenotype of flowering time suggested that AtJAC1 may negatively regulate GRP7 function. We then checked if this repression effect is based on the amount of mRNA and/or protein level change of GRP7 in AtJAC1 mutants and overexpression plants. The mRNA level of *GRP7* was slightly down-regulated in *atjac1* mutants and up-regulated in *AtJAC1*-OE lines (Fig. 4A). As well, the total protein levels of GRP7 decrease slightly in *atjac1* mutants and increase in *AtJAC1*-OE lines (Fig. 4B). However, neither transcript of AtJAC1 nor protein level showed a change in either *grp7-1* or *GRP7*-OE plants (Supplemental Fig. S6, A and B).

GRP7 is a nucleocytoplasmic shuttling protein and functions in regulating premRNA splicing within the nucleus (Lummer et al., 2011; Streitner et al., 2012). We further quantified the protein level of GRP7 in nuclear and cytoplasm fractions separately in loss- or gain-of-function AtJAC1 mutants and transgenic plants (Fig. 4B). The GRP7 protein level in the nuclear fraction was obviously elevated in *atjac1* mutants (more than 2-fold change) and reduced in *AtJAC1*-OE lines (Fig. 4B). By contrast, the cytoplasm-distributed GRP7 obviously decreased in *atjac1* mutants and increased in *AtJAC1*-OE lines (Fig. 4B). Furthermore, we used fluorescence fusion protein to visualize and quantify the distribution of GRP7-GFP in subcellular components in a transient protoplast assay. This showed that the nuclear distribution of GRP7-GFP was about 70.8% in protoplast generated from *atjac1-1* but 30.2% in that of Col, regardless of the similar total protein level of GRP7-GFP in the transient expression assay (Fig. 4C; Supplemental Fig. S6C). When *35S:AtJAC1* was introduced into *atjac1-1*, the percentage of nucleus-distributed GRP7-GFP was reduced to 24.6%, which is even significantly lower than that in Col (Fig. 4C). By contrast, the control protein GFP alone showed no significant nucleocytoplasmic distribution differences in protoplasts among Col, *atjac1-1*,

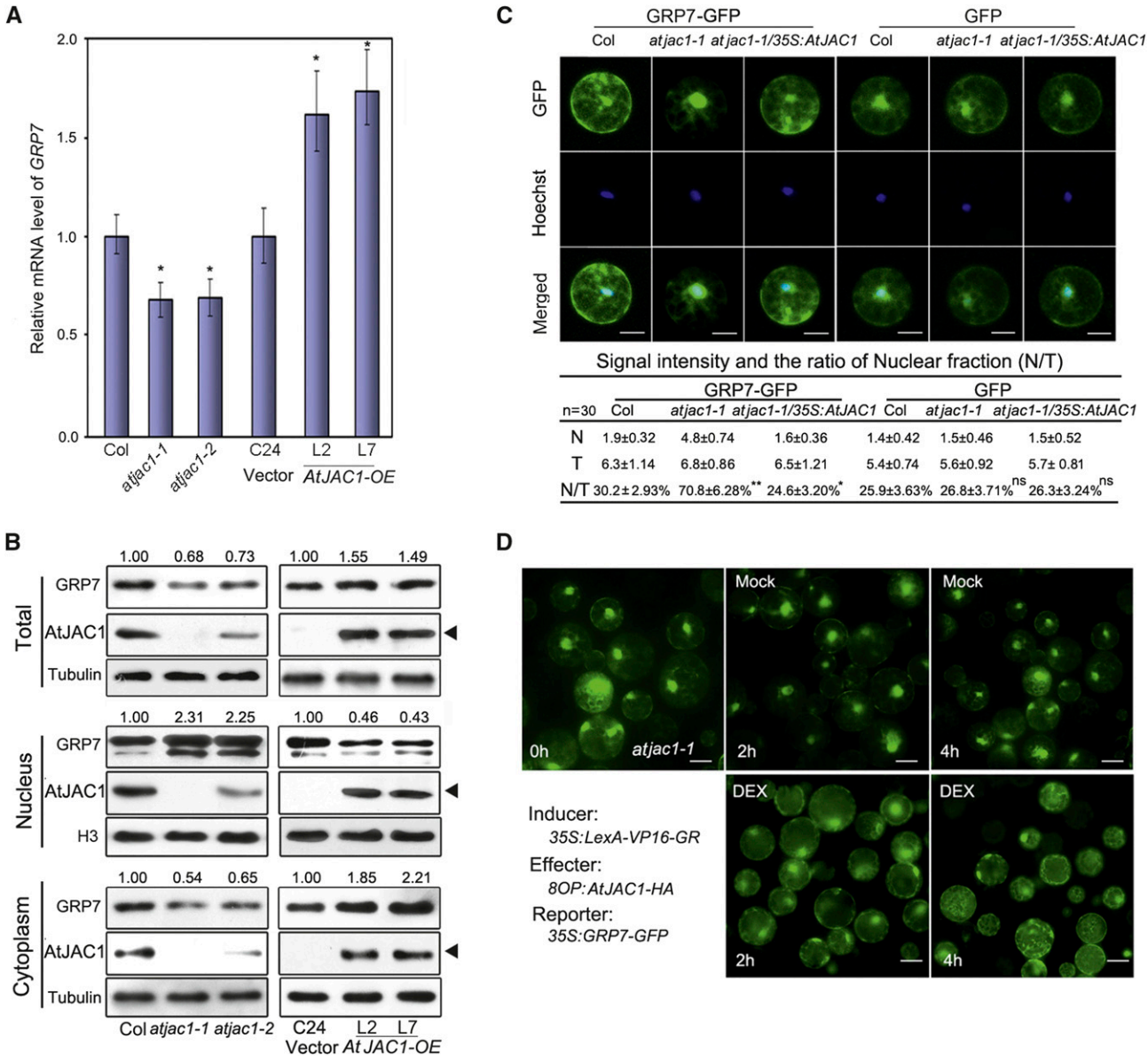

Figure 4. AtJAC1 inhibits the nuclear accumulation of GRP7. A, *GRP7* transcription was up-regulated in *AtJAC1*-OE lines and down-regulated in the *atjac1* mutant. Student's *t* test was performed; *atjac1* mutants were compared with Col, whereas *AtJAC1*-OE lines were compared with C24 (vector): *, $P < 0.05$. B, Immunoblotting of GRP7 protein in *atjac1* mutant and *AtJAC1*-OE transgenic lines. Tubulin is shown as a loading control for total protein and cytoplasmic fractions, and H3 shows loading for the nuclear fraction. Black triangles indicate AtJAC1-GFP (transgene) bands. Relative fold changes of GRP7 were quantified using ImageJ (http://rsb.info.nih.gov/ij). Experiments were repeated with three batches of independent materials. C, Quantification of GRP7-GFP distribution to the nucleus in protoplasts. The fluorescence intensities ($10^6\times$) and the ratio between the nucleus and the total (N/T) in each type of protoplast are shown below the images. N, Nuclear signal; T, total signal. Data are means ± SD of 30 individual cells of one transformation; three different transformations were done in total. Hoechst staining indicates the nucleus area. Statistical analysis was done by Student's *t* test; GRP7-GFP or GFP intensity in *atjac1-1* or *atjac1-1/35S:AtJAC1* were compared with Col: *, $P < 0.05$; **, $P < 0.01$; ns, no significant change. Bars = 10 μm. D, DEX-induced expression of AtJAC1 accelerated the spread of nucleus-localized GRP7-GFP to the cytoplasm in *atjac1-1* protoplasts. DEX, Treatment with solution containing 10 μM DEX; Mock, treatment with solution without DEX reagent. Bars = 15 μm.

and *atjac1-1* transformed with *35S:AtJAC1* (Fig. 4C). To gain more insight whether GRP7's nucleocytoplasmic distribution change is directly related to AtJAC1 or secondary effects caused by constant misexpression of AtJAC1, an inducible transient expression system (Ryu et al., 2010) was used to quantitatively increase AtJAC1 protein level. A similar phenomenon was observed in that the nucleus-localized GRP7-GFP in *atjac1-1* gradually decreased after dexamethasone (DEX)-induced expression of AtJAC1 (Fig. 4D; Supplemental Fig. S6D).

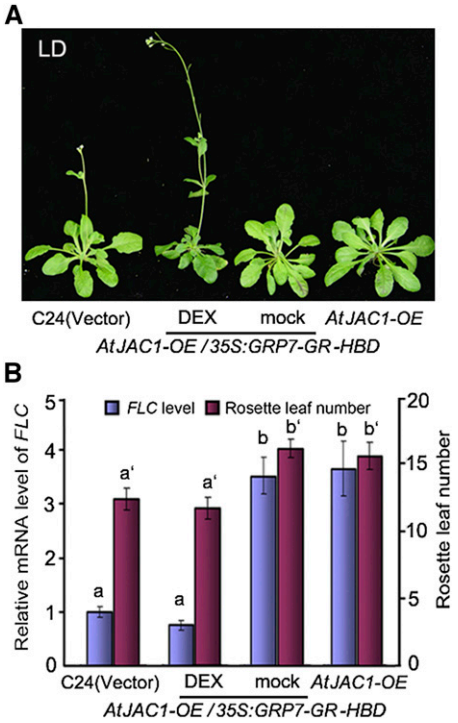

Figure 5. Nuclear accumulation of GRP7 compromises AtJAC1 function. Delayed flowering in *AtJAC1*-OE was rescued by DEX-induced nuclear accumulation of GRP7. Morphological phenotypes (A) as well as rosette leaf numbers and *FLC* mRNA levels (B) in *AtJAC1*-OE and DEX-inducible lines are shown. Statistical analysis of multiple comparisons was done by Tukey's HSD test. Letters with or without ′ represent different groups; different letters indicate statistically significant differences within groups.

Therefore, AtJAC1 negatively regulates the nuclear accumulation of GRP7.

Nuclear Accumulation of GRP7 Compromises AtJAC1 Function

Does the nuclear accumulation level of GRP7 mediate AtJAC1's regulation for flowering time? *GRP7* was in-frame fused with the GLUCOCORTICOID RECEPTOR (GR) HORMONE-BINDING DOMAIN (HBD; Schena et al., 1991) driven by the Cauliflower mosaic virus (CaMV) 35S promoter in *35S:GRP7-GR-HBD* and transformed into *AtJAC1*-OE lines (Supplemental Fig. S7A). With mock treatment (solution containing no DEX reagent), the GRP7-GR-HBD fusion protein was constitutively expressed but held in the cytoplasm by HEAT SHOCK PROTEIN90 (HSP90; Supplemental Fig. S7B). In the nuclear fraction, the endogenous GRP7 protein was lower compared with the control (transformed with empty vector) due to the overexpression of AtJAC1. Consistent with the low accumulation of GRP7 in the nucleus, the transgenic *AtJAC1*-OE$^{35S:GRP7\text{-}GR\text{-}HBD}$ lines showed delayed flowering with elevated *FLC* transcript level, similar to *AtJAC1*-OE, compared with control plants (Fig. 5, A and B). However, with the DEX treatment, GRP7-GR-HBD protein was released from HSP90 and a portion of the fusion protein was translocated into the nucleus, where the accumulation of GRP7 (endogenous GRP7 and GRP7-GR-HBD fusion protein) was increased significantly compared with that in *AtJAC1*-OE (Supplemental Fig. S7B). As expected, *AtJAC1*-OE$^{35S:GRP7\text{-}GR\text{-}HSD}$ plants rescued the delayed flowering phenotype of *AtJAC1*-OE, resulting in a similar rosette leaf number to the control plant when bolting. As well, *FLC* expression returned to the level of the control (Fig. 5, A and B). Therefore, the nuclear accumulation level of GRP7 coordinates the regulation of flowering by AtJAC1.

GRP7 Directly Binds *FLC* Antisense premRNA through a Conserved Motif

To find the direct target of GRP7, systematic evolution of ligands by exponential enrichment (SELEX; Tuerk and Gold, 1990; Xiao et al., 2014) was used to screen for the RNA-binding preference of GRP7. The most enriched RNA motif, $U/G^1N^2N^3U^4U/G^5N^6U^7G^8G^9N^{10}U/G^{11}N^{12}N^{13}U/G^{14}U/G^{15}$ (E value of 7.4e-042), was calculated by MEME2 (Bailey et al., 2009) with the input sequences from the SELEX screening (Fig. 6A; Supplemental Table S2). RNA-electrophoresis mobility shift assay (EMSA) data showed that GRP7 could bind this RNA motif in vitro (Fig. 6B). Point mutation of specific nucleotides (U to A and G to A) suggests that U^4U/G^5 and $U^7G^8G^9$ are necessary for the binding, whereas $U/G^1U/G^{11}$ and $U/G^{14}U/G^{15}$ contribute less (Supplemental Fig. S8A). Swapping of U to G or G to U at positions 4, 5, 7, 8, and 9 of this motif reduced the binding intensity of GRP7 in the RNA-EMSA (Supplemental Fig. S8B). This suggested that the sequence itself contributes more to the binding of GRP7 than the nucleotide composition.

Sequence analysis showed the two putative GRP7-binding motifs located closely in intron 6 of *FLC*, on opposite strands (Fig. 6C; Supplemental Table S3). RNA-EMSA indicated that GRP7 could bind both sense and antisense RNA probes in vitro (Fig. 6D). We used in vivo RNA immunoprecipitation (RIP) followed by reverse transcription (RT)-PCR to identify the binding status of GRP7 at the *FLC* locus in planta. Point mutation of $R^{49}Q$ (Arg to Gln at the 49th amino acid) in the RNA recognition motif domain of GRP7 dramatically reduced its RNA-binding ability (Schöning et al., 2007), which was used as a negative control for the RNA-binding specificity of GRP7. After IP with GRP7 antibody, the coimmunoprecipitated RNA pools were reverse transcribed with adaptor primer and further amplified with specific primers as indicated (Supplemental Fig. S9). Consistent with a previously reported EMSA in vitro (Schöning et al., 2007), the GRP7 and GRP8 untranslated region (UTR) was enriched in the IP-GRP7 sample from Col but reduced in *grp7-1* transformed with *pGRP7:GRP7*^{R49Q} and not

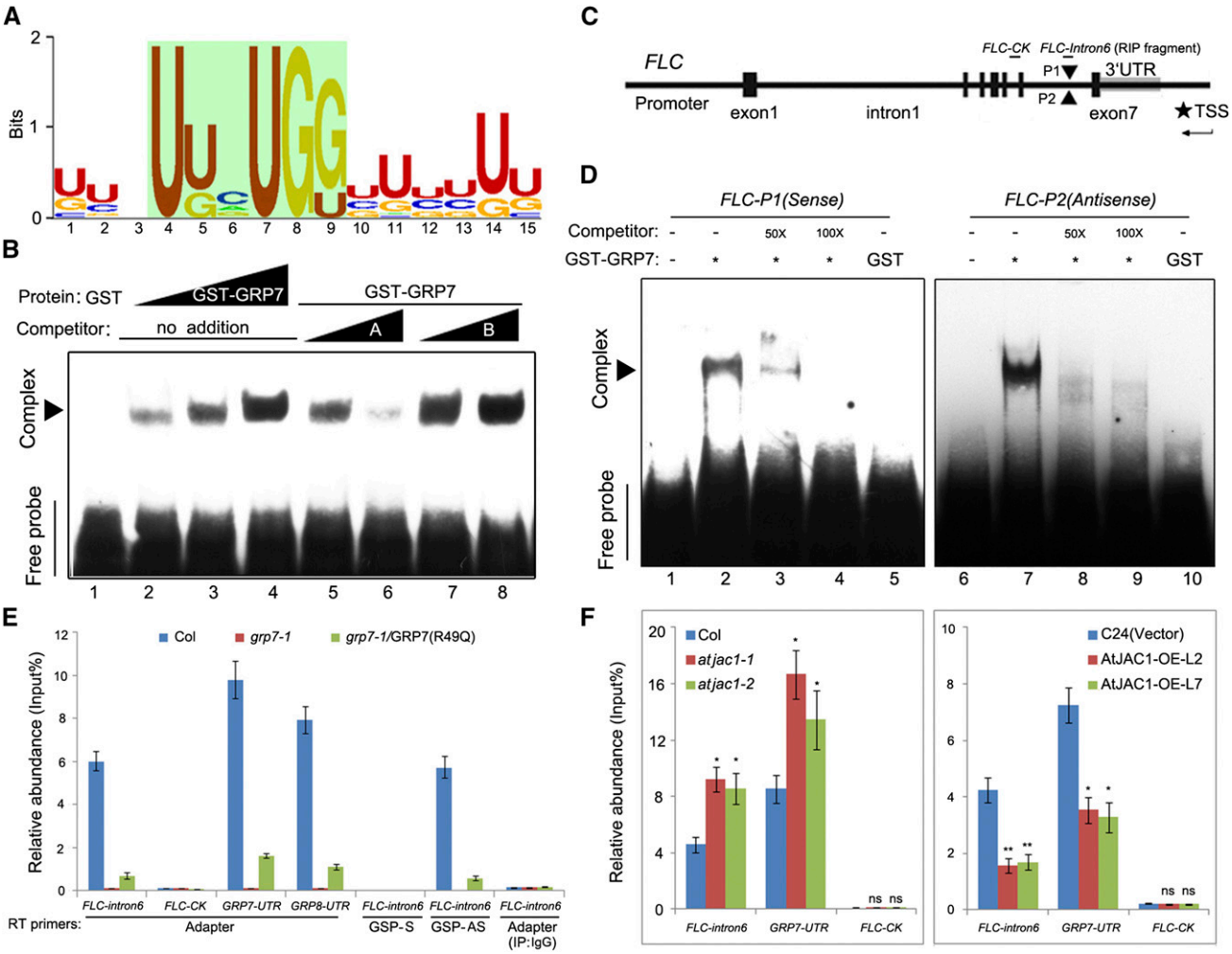

Figure 6. GRP7 directly binds *FLC* antisense premRNA through a conserved motif. A, The most significantly enriched RNA-binding motif of GRP7 screened by SELEX and analyzed by MEME2. B, RNA-EMSA to confirm the binding of GRP7 to the motif screened out by SELEX in vitro. Competitor A was a non-biotin-labeled GRP7-binding motif, and competitor B was a nonrelevant RNA fragment without biotin labeling. Sequences of individual oligonucleotides are listed in the supplemental sheet. C, Schematic diagram of the positions of putative GRP7-binding motifs in the *FLC* genomic sequence. Gene structure is as indicated. P1 and P2, Two putative GRP7-binding sites in *FLC* intron 6 with opposite directions; TSS, transcription start site for antisense *FLC*. D, GRP7 binds to *FLC* sense and antisense RNA probes in RNA-EMSA in vitro. Competitors are non-biotin-labeled RNA fragment *FLC-P1* or *FLC-P2*. E, RIP followed by qPCR to confirm the binding of GRP7 to antisense *FLC* premRNA in vivo. *FLC*-intron6, *FLC* sense or antisense premRNA fragment containing putative GRP7-binding sites, with position indicated in C; *FLC*-control check fragment (*FLC*-CK), *FLC* premRNA fragment containing no GRP7-binding sites as a negative control, with position indicated in C; GSP, gene-specific primer. The GRP7/GRP8-UTR fragment served as a positive control, and *grp7-1* transformed with pGRP7:GRP7($R^{49}Q$) served as a negative control for GRP7-binding activity. F, The binding of GRP7 to *FLC* antisense premRNA was altered in *atjac1* mutants and *AtJAC1*-OE plants compared with controls. Adaptor primers were used for RT after determining the RNA pool with IP. Data shown in E and F are means ± SD of three parallel samples from one replicate, and three biological repeats were performed. Statistical analysis was done by Student's *t* test: *, $P < 0.05$; **, $P < 0.01$; ns, no significant change.

detected in *grp7-1*, suggesting that the RIP assay works in vivo (Fig. 6E; Supplemental Fig. S10). The *FLC-intron6* fragment, which contained the two putative binding motifs, was indeed enriched in Col but hard to detect in *grp7-1* or *grp7-1* transformed with *pGRP7:GRP7*^{R49Q}, with no detection in Col using a nonrelated IgG for IP. By contrast, the *FLC-CK* fragment in intron 5 lacking the GRP7-binding motif was not detected in Col (Fig. 6, C and E; Supplemental Fig. S9). Primers complemented to sense or antisense strands specifically were then used to substitute for the adaptor primer when generating the first-strand complementary DNA (cDNA) from the RNA pool CoIP with GRP7 antibody. The *FLC-intron6* fragment could only be detected in Col when using the primer complemented to antisense RNA (Fig. 6E; Supplemental Fig. S10). Thus, GRP7 binds directly to *FLC* antisense premRNA in vivo.

As expected, we find more coimmunoprecipitated *FLC* antisense premRNA with GRP7 in the background of *atjac1* mutants compared with wild-type Col by RIP-qPCR (Fig. 6F). By contrast, less was detected in *AtJAC1*-OE transgenic plants as compared with the control (C24 transformed with vector; Fig. 6F).

GRP7 and AtJAC1 Influence the RNA Processing of *FLC* Antisense Transcripts (*COOLAIR*)

The consequence of directly binding GRP7 to *FLC* antisense premRNA was analyzed. Naturally occurring long noncoding RNA antisense transcripts, named *COOLAIR*, originate from the promoter adjacent to the *FLC* 3′ UTR and consist of two classes, terminating at proximal (sense intron 6) or distal (sense promoter) sites; each class contains several subclasses of alternative splicing variants (Swiezewski et al., 2009; Hornyik et al., 2010; Helliwell et al., 2011; Fig. 7A). Of note, the GRP7-binding site is close to the polyadenylation site of the proximal type *COOLAIR*, where the RNA-binding factor FCA and the 3′ RNA processing factors Cst64 and Cst77 are also associated (Liu et al., 2007, 2010). Therefore, we investigate whether loss of *GRP7* function could affect the targeted 3′ processing and polyadenylation pattern of *COOLAIR*. Compared with wild-type Col, the *grp7-1* mutant had elevated levels of total antisense transcripts (Fig. 7B). In addition, the relative abundance of proximal type ASI (Type I/Total) was decreased in *grp7-1*, whereas relative distal type ASII (Type II/Total) was increased (Fig. 7B), which also matches the previous report in *fca-9* (Liu et al., 2007, 2010).

Alternative polyadenylation of the *COOLAIR* transcripts has been shown to trigger changes in histone methylation status at the *FLC* locus (Liu et al., 2007). Therefore, we checked whether *grp7* influenced H3K4 dimethylation at the *FLC* gene body. Mutant *grp7-1* increased H3K4me2 in the body of the gene downstream of the proximal *COOLAIR* poly(A) site (Fig. 7C). In addition, the H3K27me3 level decreased in the gene body of *FLC* in the *grp7-1* mutant (Fig. 7D). Moreover, relative changes of different types of *FLC* antisense transcripts and histone modification levels (H3K4me2 and H3K27me3) at *FLC* gene body regions were observed in *AtJAC1*-OE plants, with contrivance for *atjac1* mutants (Fig. 7, B–D). It has been shown that the *COOLAIR* amount as well as the ratio of proximal type over distal type increased during the vernalization process and led to reductions of H3K36me3 and H3K4me3 at the *FLC* locus (Csorba et al., 2014; Yang et al., 2014), and we further checked these two histone modification marks. Increased H3K4me3 and H3K36me3 levels around the transcription start site of the *FLC* locus was observed in *grp7-1* mutant and *AtJAC1*-OE lines, whereas reduction of those histone modifications was found in *atjac1* mutants (Supplemental Fig. S11). Thus, AtJAC1 and GRP7 may be involved in *FLC* transcript level regulation by influencing the processing of *COOLAIR* and related histone modification dynamics.

Competition of GRP7 Binding Influences *COOLAIR* Process and Flowering

Is the RNA processing change of *COOLAIR* associated with direct binding of GRP7? To address this, a DNA fragment containing 12 repeats of the GRP7-binding site (GRP7BS) driven by the CaMV 35S promoter was transformed into Col, which could generate bait RNA fragments to compete the binding of endogenous GRP7 (Supplemental Fig. S12A; Supplemental Table S4). As a control, a DNA fragment of the same size with a mutation at the consensus site ($U^4U/G^5U^7G^8G^9$) of the GRP7-binding motif (GRP7BSm) was transformed in parallel to Col (Supplemental Fig. S12B; Supplemental Table S4). RIP followed by RT-qPCR revealed that the endogenous GRP7 strongly bound to this artificial bait RNA fragment, whereas decreased binding was seen with the *FLC* antisense premRNA fragment (*FLC-intron6*) in Col^{GRP7BS} transgenic plants compared with Col (Fig. 8A). Consistently, GRP7-UTR RNA fragments also showed a reduced enrichment in the coimmunoprecipitated RNA pool of anti-GRP7 (Fig. 8A). In contrast, GRP7 rarely bound to the *GRP7BSm* RNA fragments, and there was no difference between Col and $Col^{GRP7BSm}$ plants with respect to GRP7 binding to either *FLC* antisense premRNA or GRP7/8-UTR RNA fragments (Fig. 8A). The endogenous *GRP7* mRNA level increased in Col^{GRP7BS}, which is likely caused by the autonegative regulation machinery of GRP7 (Staiger et al., 2003; Fig. 8B). Consistent with the reduced binding of GRP7 to *FLC* antisense premRNA, the relative abundance of different poly(A) types of *COOLAIR* transcripts showed similar changes in Col^{GRP7BS} transgenic plants to those in *grp7-1*, with increased total *COOLAIR* production and reduced proximal polyadenylation (type I) site usage (Fig. 8B). Meanwhile, the histone modification status of H3K4me2 and H3K27me3 at the *FLC* gene body also was altered in Col^{GRP7BS} as in *grp7-1* compared with Col (Fig. 8C). As expected, the total amount of *FLC* sense transcript level increased (Fig. 8B), with concomitant delayed flowering, in Col^{GRP7BS} compared with Col (Fig. 8D). By contrast, in $Col^{GRP7BSm}$ plants, neither *COOLAIR* polyadenylation, histone modification, nor flowering time change was observed compared with Col (Fig. 8, B–D).

Therefore, the binding of GRP7 to *FLC* antisense premRNA influences its RNA processing and, consequently, flowering time.

DISCUSSION

JACALIN-RELATED LECTIN Regulates Flowering in Both Dicot and Monocot Plants

JACALIN-RELATED LECTIN (JRL) belongs to one of the superfamily of plant lectins, with numerous members among different plant species. There are 48 JRL proteins in Arabidopsis (Nagano et al., 2008), 31 in rice (Jiang et al., 2010), and 67 in wheat (Song et al., 2013b). Beyond the classic lectins (Lannoo and Van

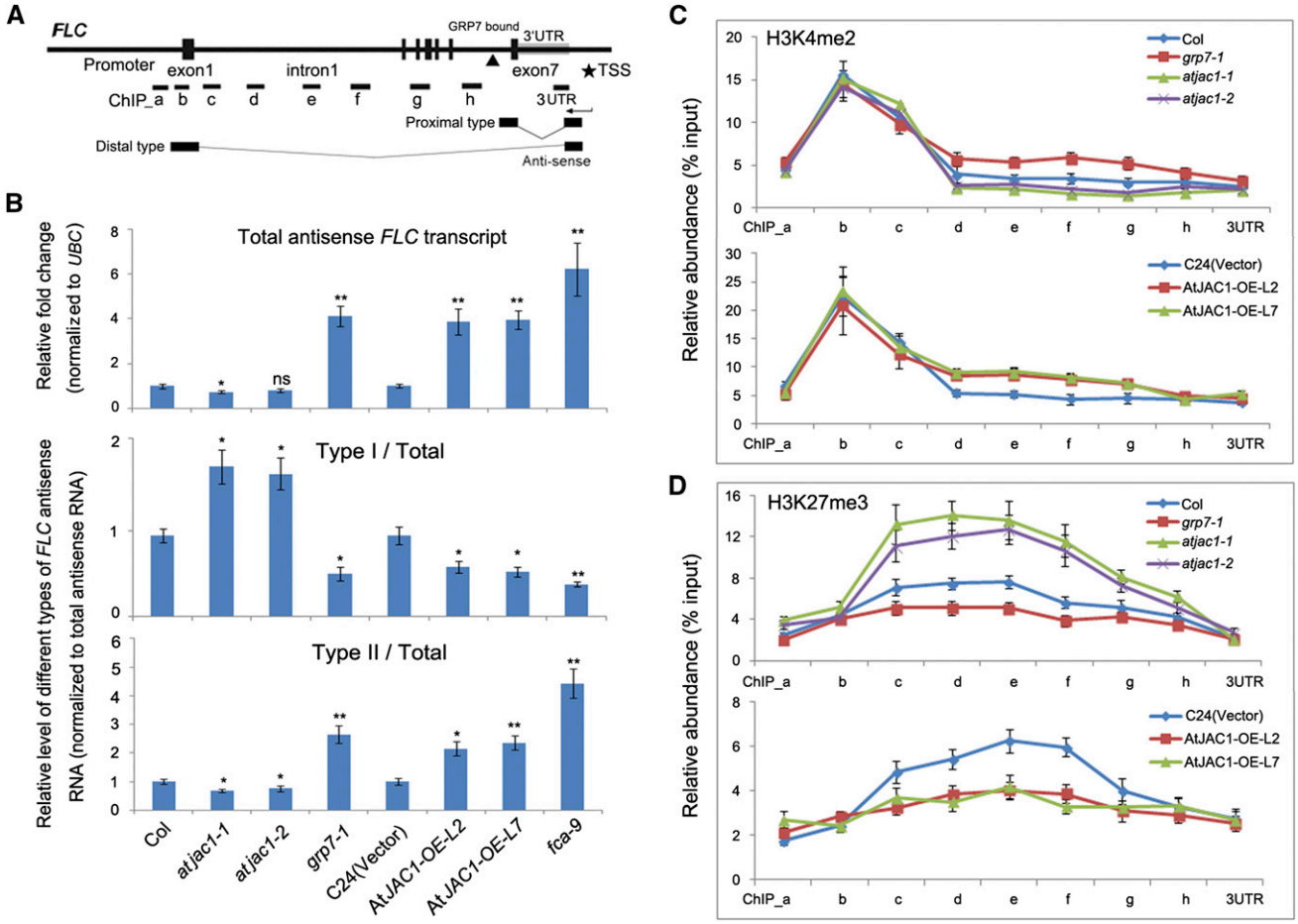

Figure 7. GRP7 and AtJAC1 influence the RNA processing of *COOLAIR* and histone modification within the *FLC* gene body. A, Diagram of *FLC* gene structure and antisense transcripts. The black triangle indicates the GRP7-binding site. PCR-amplified fragments for chromatin immunoprecipitation (ChIP) in C and D are indicated as ChIP_a to 3UTR. B, Relative expression of total antisense mRNA (normalized to *UBC*) as well as relative ratio of proximal (type I) and distal (type II) antisense transcripts (normalized to total antisense transcripts) in *atjac1*, *grp7-1*, and *fca-9* mutants and *AtJAC1*-OE plants compared with controls. In total, three biological repeats were performed. Statistical analysis was done by Student's *t* test; *atjac1* mutants, *grp7-1*, and *fca-9* were compared with Col, whereas *AtJAC1*-OE lines were compared with C24 (vector): *, $P < 0.05$; **, $P < 0.01$; ns, no significant change. C and D, Histone modification change (H3K4me2 [C] and H3K27me3 [D]) at the *FLC* locus in *atjac1*, *grp7-1* mutants, and *AtJAC1*-OE plants compared with controls. The *y* axis shows the relative abundance of ChIP sample compared with input. Data are means ± SD of three parallel samples from one replicate, and three biological repeats were performed.

Damme, 2010), as defined by characteristics such as high expression in storage organs, distribution in extracellular compartments, and recognition of exogenous carbohydrate or glycoprotein, increasing numbers of inducible JRLs were reported to be important in the regulation of plant development as well as biotic and abiotic stress responses (for review, see Lannoo and Van Damme, 2010). Our data here revealed that the Jacalin-lectin AtJAC1/JRL35 (Nagano et al., 2008) regulates the transition of flowering in Arabidopsis. Mutants of *atjac1* were early flowering, whereas overexpression of *AtJAC1* led to delayed flowering (Fig. 1). We reported previously that VER2, a Jacalin domain-containing lectin, is also involved in the regulation of the flowering transition in wheat (Yong et al., 2003; Xiao et al., 2014). In contrast to VER2, a promoter of flowering transition in wheat, AtJAC1 is a flowering repressor in Arabidopsis. VER2 is induced by cold temperature, and its function in the regulation of flowering is mainly dependent on the vernalization pathway, whereas AtJAC1 has high basal expression under normal growth conditions (Supplemental Fig. S1F) and regulates flowering through the autonomous pathway instead of vernalization (Fig. 1). VER2 is a positive regulator of TaVRN1, an AP1-like MADS box transcription factor that mediates the vernalization-accelerated flowering transition in wheat (Xiao et al., 2014). Here, we find that AtJAC1 participates in flowering control through the regulation of the transcript of *FLC*, an integrator of the vernalization and autonomous pathways (Fig. 2). Interestingly, FLC-like repressors were also shown in cereals to mediate vernalization-regulated flowering (Ruelens et al., 2013). To conclude, JRL could

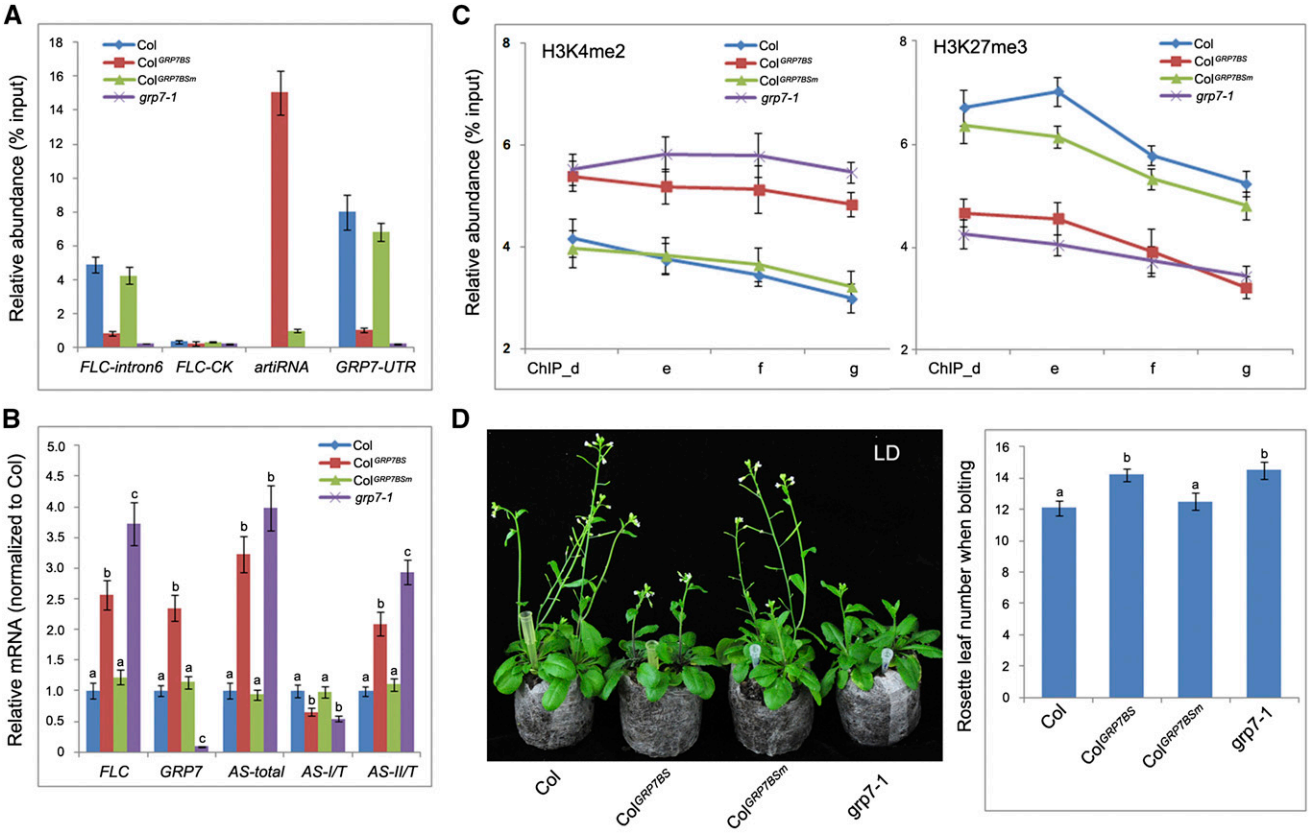

Figure 8. Reducing GRP7 binding influences *COOLAIR* process and flowering. A, Competing the binding of GRP7 to its target RNA by artificial RNA fragments reduced the binding of GRP7 to *FLC* antisense premRNA. RIP was followed by qPCR to check the relative abundance of GRP7 binding at *FLC-intron6*, *FLC-CK*, *GRP7-UTR*, and artificial RNA fragments. Adaptor primers were used in RT. Col^{GRP7BS}, Col with abundant expression of an RNA fragment containing the GRP7-binding site; Col^{GRP7BSm}, Col with abundant expression of an RNA fragment containing a mutated GRP7-binding site. B, Relative expression level of sense *FLC*, *GRP7*, and different polyadenylated *FLC* antisense (AS) mRNAs in Col, artificial RNA transgenic plants, and the *grp7-1* mutant. C, Histone modification change (H3K4me2 and H3K27me3) at *FLC* gene body regions (ChIP_d, e, f, and g as in Fig. 7A) in Col, artificial RNA transgenic plants, and the *grp7-1* mutant. D, Flowering time (morphology, left; rosette leaf number when bolting, right) changes in Col, artificial RNA transgenic plants, and the *grp7-1* mutant. Tukey's HSD test was used for B and D, and different letters within the same genetic background indicate statistically significant differences.

regulate the flowering transition in both monocot and dicot plants, although the exact players and regulation models in different species may vary.

Jacalin-Lectins Interact with RNA-Binding Proteins and Regulate Their Function

It is intriguing how JRLs participate in the regulation of gene expression. In wheat, the Jacalin-lectin domain-containing protein VER2 could bind to the *O*-GlcNAcylated RNA-binding protein TaGRP2 during the process of vernalization through the high-affinity association of VER2 to the GlcNAc side chain. Their interaction leads to the dissociation of TaGRP2 from *TaVRN1* premRNA and releasing the inhibition of transcription (Xiao et al., 2014). It suggests an important input of *O*-GlcNAc signaling in shaping plant development meditated by lectin and target proteins (Liu et al., 2015). Unlike VER2, AtJAC1 shows highly specific recognition of Man, Rib, and Glc instead of *N*-acetyl-D-glucosamine (Supplemental Table S1; Supplemental Fig. S1E). Accordingly, it is unlikely that AtJAC1 could bind an *O*-GlcNAc-ylated protein as VER2. Although the specific recognition of carbohydrate is a fundamental character of lectins, other studies indicate that many plant lectins could also interact with small molecules and peptides independent of their carbohydrate-binding properties (for review, see Komath et al., 2006). Evidence from CoIP and BiFC assays indicated that AtJAC1 could also interact with GRP7 in Arabidopsis (Fig. 3). Whether this interaction is mediated by the carbohydrate-binding property of AtJAC1 needs to be analyzed further. Nevertheless, the interaction between JRL and RNA-binding proteins seems to be conserved in both monocots and dicots.

Like the inducible lectins (Lannoo and Van Damme, 2010), AtJAC1 is a nucleocytoplasmic protein (Supplemental Fig. S4A). As well, GRP7 could also

localize in both nucleus and cytoplasm (Supplemental Fig. S4A). However, interaction between AtJAC1 and GRP7 occurs only in the cytoplasm, based on the BiFC and CoIP data presented here (Fig. 2). This is different from the case of VER2 and TaGRP2 in wheat, where interaction occurs in both nucleus and cytoplasm (Xiao et al., 2014). Of note, immunoblot data indicate that there are two bands of GRP7 in the nuclear fraction but only one in the cytoplasm (Figs. 3 and 4). The two bands might be related to posttranslational modification or alternative splicing and possibly contribute to the specific subcellular interaction with AtJAC1. GRP7 was shown to shuttle between nucleus and cytoplasm (Lummer et al., 2011), which may be linked to its multiple functions in RNA processing. Immunoblot data and transient fluorescence reporter assays suggest that AtJAC1 is involved in the regulation of GRP7's distribution between nucleus and cytoplasm. With high expression of AtJAC1, GRP7 was detained in the cytoplasm, whereas reduced expression of AtJAC1 caused an accumulation of GRP7 in the nucleus (Fig. 4). In addition, a DEX-inducible assay suggests that the nuclear accumulation of GRP7 rescued the developmental defects and altered gene expression caused by the overexpression of *AtJAC1* (Fig. 5). Thus, AtJAC1 could participate in the developmental program through regulating the nucleocytoplasmic distribution of GRP7. Furthermore, the subcellular distribution of GRP7 provides a novel regulation of GRP7's function besides its well-known transcriptional autonegative feedback machinery and posttranslational modifications such as ADP-ribosylation and methylation on Arg (Staiger et al., 2003; Fu et al., 2007; Deng et al., 2010).

GRP7 Binds Directly to *COOLAIR* premRNA and Affects Its Processing

Although GRP7 was reported to regulate the *FLC* transcript level and influence flowering time (Streitner et al., 2008), the direct link between GRP7 and *FLC* is still unclear. Here, we identified a GRP7-binding RNA motif as $U/G^{1}N^{2}N^{3}U^{4}U/G^{5}N^{6}U^{7}G^{8}G^{9}N^{10}U/G^{11}N^{12}N^{13}U/G^{14}U/G^{15}$, with the core consensus motif of UUNUGG. Sequence alignment showed two GRP7-binding motifs present on opposite strands of the last intron of the *FLC* gene, where important regulatory factors are associated (Liu et al., 2007, 2010). GRP7 could bind both RNA probes in vitro; however, only the antisense premRNA of *FLC* could be coimmunoprecipitated with GRP7 in vivo (Fig. 6). The data presented here provide evidence of a direct link between GRP7 and *FLC* transcript regulation. They also suggests that, besides the sequence conservation, other regulatory events like RNA secondary structure may also be required in facilitating the association of RNA-binding proteins to their target (Brown et al., 2009).

At the *FLC* locus, a group of long noncoding antisense transcripts named *COOLAIR* generates from the 3′ UTR (Swiezewski et al., 2009). It is induced by vernalization but also exists in warm conditions (Swiezewski et al., 2009). Although its function in the vernalization-triggered silencing of *FLC* expression is still under debate (Helliwell et al., 2011; Csorba et al., 2014), numerous data indicate that *COOLAIR* has an important role in mediating *FLC* expression in nonvernalized plants (Liu et al., 2010; Marquardt et al., 2014; Wang et al., 2014). *COOLAIR* consists of two major types with alternative polyadenylation and alternative splicing (Swiezewski et al., 2009; Hornyik et al., 2010). The relative ratio of these two types (type I with proximal polyadenylation in the last intron of *FLC* and type II with distal polyadenylation in the promoter of *FLC*) regulates the amount of *FLC* sense transcript in a way linked to dynamic histone modification at the *FLC* gene body region (Liu et al., 2007; Csorba et al., 2014). The processing of *COOLAIR* is regulated by RNA-binding proteins like FCA, FPA, and RNA 3′ processing factors like FY, CstF77, and CstF64 (Hornyik et al., 2010; Liu et al., 2010). In addition, the promoter of *COOLAIR* is regulated by the presence of an R loop, which could reduce *COOLAIR* expression upon stabilization by homeodomain protein (Crevillén et al., 2013; Sun et al., 2013). Here, we find that GRP7 could directly bind *COOLAIR* premRNA just downstream of the polyadenylation site of proximal class *COOLAIRs* (Fig. 6). Furthermore, the total amount of *COOLAIR*, as well as the relative abundance of the proximal class *COOLAIR*, were altered in the *grp7-1* mutant (Fig. 7). The effect of GRP7 on *COOLAIR* processing is likely to rely on the direct binding. To support this view, we find that when overexpressing an RNA fragment containing a multimer of GRP7-binding motifs in wild-type plants, it could phenotypically mimic the *grp7-1* mutant at both the morphological level (flowering time) and the molecular level (total *COOLAIR* and *FLC* transcript levels as well as the relative abundance of proximal *COOLAIR* transcript). In contrast, overexpression of the RNA fragment containing the mutated GRP7-binding motifs behaves like the wild type (Fig. 8).

Our data suggested that GRP7 may be involved in the regulation of *COOLAIR* processing, such as facilitating the poly(A) site chosen and/or the generation of *COOLAIR*. RNA-binding proteins frequently interact with each other in different RNA processing steps. Interestingly, there is no physical interaction between GRP7 and multiple known factors in the regulation of poly(A) site selection (Supplemental Fig. S13). GRP7 was suggested to have a function in premRNA splicing, particularly in affecting the splicing site choice (Streitner et al., 2012). Alternative splicing of both proximal and distal *COOLAIR* can quantitatively modulate *FLC* sense transcript expression through a feedback mechanism linking *COOLAIR* processing to *FLC* gene body histone demethylation (Marquardt et al., 2014). It is possible that GRP7 could participate in the alternative splicing of *COOLAIR* through direct binding. In addition, we find that GRP7 could interact with the nuclear exosome component RRP6 like protein1 protein in a yeast two-hybridization screening study (Supplemental Fig. S14).

The latter protein has been reported to influence *FLC* antisense transcript generation (both *COOLAIR* and a novel antisense transcript, *ASL*; Shin and Chekanova, 2014).

Jacalin-Lectin AtJAC1 May Have Broad Function through the Regulation of GRP7-Manipulated RNA Processing

Of interest, the total *COOLAIR* expression level and relative proximal *COOLAIR* abundance also changed in *atjac1* mutants and *AtJAC1*-OE lines, indicating that AtJAC1 could take part in RNA processing regulation through the manipulation of GRP7's nuclear accumulation. Besides the dynamic expression profile during different developmental stages, AtJAC1 also shows elevated or reduced expression at the mRNA or protein level upon hormone treatments (JA [León et al., 1998], ethylene [Tamaoki et al., 2008], and Brassinosteroid [Tang et al., 2008]) and environmental cues (light [Piippo et al., 2006], cold [Bae et al., 2003], wounding [León et al., 1998], and pathogens [Thilmony et al., 2006]). This suggests that AtJAC1 may have broad function in plant development and stress responses. Coincidentally, GRP7 also responds to multiple endogenous and environmental cues, such as high salinity, cold, or osmotic stress (Kim et al., 2008), pathogens (Fu et al., 2007), and hormones (Cao et al., 2006; Hackmann et al., 2014). The working model we present here for AtJAC1 and GRP7 in the regulation of flowering could also be adapted to other developmental aspects and stress-response scenarios. It will be interesting to study the transcriptome profile change upon misexpression of AtJAC1 combined with the GRP7 genome-wide binding target RNA data.

MATERIALS AND METHODS

Plant Materials and Treatment

Arabidopsis (*Arabidopsis thaliana*) ecotypes Col and C24 were used as the genetic backgrounds of mutants and transgenic lines, respectively. Mutants *atjac1-1* (SALK_000461), *atjac1-2* (SALK_112556), *At3g16460* (SALK_028332), *grp7-1* (SALK_039556), and *grp8* (SALK_007963) were ordered from the SALK T-DNA collection (Alonso et al., 2003); *flc-20* was described previously (Helliwell et al., 2002). Plants were grown at 22°C under LD (16 h of light/8 h of dark) or SD (8 h of light/16 h of dark) conditions. Vernalization and GA treatments were as described (Bastow et al., 2004; Lim et al., 2004). Flowering time was measured as the number of rosette leaves when bolting. For DEX treatment, seedlings of *grp7-1* and Col transformed with 35S:GRP7-GR-HBD were sprayed with a solution containing 10 μM DEX (Sigma), 0.01% (v/v) ethanol, and 0.015% (v/v) Silwet L-77 at the shoot apex region every 3 to 4 d until bolting.

Transgenic Plants

The pBI121 plasmids carrying *35S:AtJAC1-GFP* and *35S:GFP* were transformed into *Agrobacterium tumefaciens* strain GV3101 separately, and the resulting bacteria were used to transform Arabidopsis ecotype C24. The *AtJAC1*-OE plants were selected on one-half-strength Murashige and Skoog (MS) medium containing 40 μg mL^{-1} kanamycin. The pSN1301-GRP7 plasmid was transformed in the Col ecotype to generate *GRP7*-OE plants, with selection by 25 mg mL^{-1} hygromycin. The *35S:GRP7-GR* construct was made by creating a translational fusion between the GRP7 cDNA and the ligand-binding domain of the rat GR under the promoter of CaMV 35S. It was transformed in *AtJAC1*-OE lines to test the DEX-inducible nuclear accumulation of GRP7's effects on flowering. The transformants were selected on one-half-strength MS medium with 30 μg mL^{-1} Basta. DNA fragments containing the GRP7-binding motif or mutated versions of GRP7-binding motifs were synthesized, cloned into the binary vector pSN1301 plasmid, and transformed in Col in *A. tumefaciens* strain GV3101. The transformants were selected on one-half-strength MS medium with 20 μg mL^{-1} hygromycin.

Plasmids and Antibodies

All plasmids and antibodies used are described in Supplemental Text S1.

Real-Time PCR

Total RNA samples were treated with Turbo DNA-free (Ambion) to remove any contaminating genomic DNA. The first-strand cDNA was prepared using the SuperScript III First Strand Synthesis System (Invitrogen) using oligo(dT) or gene-specific primers. qPCR was performed on the Mx3000p (Agilent) using SYBR Green reagent (Toyobo). Every PCR was performed using at least three biological replicates with three technical repeats. qPCR data were first normalized to *UBC* as reported (Liu et al., 2010) and then normalized to either Col (for *atjac1-1*, *atjac1-2*, and *grp7-1*) or C24 transformed with empty vector (for *AtJAC1*-OE-L2/L7). For measuring different polyadenylated *COOLAIR*s, oligo (dT) primer was used for RT, and then specific primers for different types of *COOLAIR* were used for qPCR analysis as reported previously (Liu et al., 2010). qPCR was performed in triplicate for each sample. Average values were normalized to the expression of total *COOLAIR*. The primers used are listed in the supplemental sheet.

Subcellular Fractionation

Nuclear and cytoplasmic protein fractions were isolated as described (Xiao et al., 2014). Briefly, plant material was ground in extraction buffer and filtered through Miracloth (Calbiochem) to obtain the total extract and then centrifuged at 3,000*g*. The supernatant (cytoplasmic fraction) was removed and stored on ice until use. The pellets were further washed with a resuspension buffer and then reconstituted as the nuclear fraction. Immune detection of histone H3 and tubulin was used to confirm the fractionation of nucleus and cytoplasm, respectively.

Protein Interaction Analysis

CoIP assays were performed as described (Xiao et al., 2014). Briefly, FLAG-AtJAC1 was coexpressed with GRP7-GFP or GFP in tobacco (*Nicotiana tabacum*) leaves, and after 2 to 3 d, plant material was harvested and ground in native protein extraction buffer, filtered, and centrifuged. The supernatant was incubated with anti-GFP antibody or anti-AtJAC1 antibody coupled to protein A/G Sepharose beads (Millipore), the beads were washed four times with wash buffer, and bound proteins were eluted with elution buffer containing 2% (w/v) SDS for immunoblotting with FLAG or anti-GRP7 antibody. BiFC assays were as described (Xiao et al., 2014). Briefly, constructs for the expression of AtJAC1-YFP^{NE}, GRP7-YFP^{CE}, AtJAC1-YFP^{CE}, and GRP7-YFP^{NE} were generated and cotransformed into Arabidopsis protoplasts. YFP fluorescence was visualized with a confocal scanning microscope 40 to 48 h after infiltration.

Protoplast Transient Expression

Transient expression of *35S:GRP7-GFP*, *35S:AtJAC1-GFP*, *35S:GFP*, *35S:VP16-GR*, and *8OP:AtJAC1* in protoplasts from Col or *atjac1-1* was as described (Yoo et al., 2007). Briefly, 4×10^4 mesophyll protoplasts were isolated from 4-week-old seedlings and transformed with 10 to 15 μg of purified plasmid DNA. Transformed protoplasts were incubated under weak light at 22°C. For DEX treatment, 10 μM DEX was added to the protoplasts 8 h after transfection and incubated for 2 to 4 h. GRP7-GFP, AtJAC1-GFP, or GFP signal was observed by fluorescence microscopy (Fig. 4D) or confocal microscopy (Fig. 4C; Supplemental Fig. S4A; Leica TCS SP5).

Confocal Microscopy Observation and Quantification of Fluorescent Protein Signal

GFP/YFP fluorescence was visualized using a confocal microscope (Leica TCS SP5) with an argon laser (488 nm); the autofluorescence of chloroplasts also

appeared at this excitation wavelength. Hoechst fluorescence was excited by a laser at 405 nm. Images of fluorescence at different layers along the z-axis were collected and overlaid to give a full view of the GFP/YFP signal. Hoechst fluorescence and bright field were captured at their proper layers of the z-axis to show the positions of the nucleus and whole protoplast cells, respectively. Quantification of the fluorescent protein signal was performed using ImageJ (http://rsb.info.nih.gov/ij). To calculate the ratio of the nucleus to total signals of GRP7-GFP for each cell, nucleus positional area (indicated by Hoechst inflorescence) and GFP signal intensity were measured and divided by the total GFP signal of the whole cell. A representative image of each transformant is shown in Figure 4C. The numbers indicate the relative nucleus-distributed ratio of GRP7-GFP or GFP. This experiment was carried out for three biological replicates, with each sample consisting of at least 30 cells analyzed, and the signal intensity is presented as means ± SD.

RNA-EMSA

RNA probes were generated in vitro by the use of a T7 high-yield transcription kit (Thermo). Biotin was added to the 3′ end of RNA probes using the RNA 3′ End Biotinylation kit (Pierce). RNA-EMSA was performed according to the kit instructions (Pierce). Purified RNase-free GST-GRP7 was used. All probe sequences, including those for mutations, are listed in the supplemental sheet. Typically, 20 to 50 pM protein and 0.1 pM probe were used in this study.

SELEX

SELEX was performed as described previously (Xiao et al., 2014). The RNA library was reduced to 20 random nucleotides. The oligonucleotide template and primers are listed in the supplemental sheet. The in vitro-transcribed RNA library was incubated with GST-GRP7 fusion proteins bound to glutathione Sepharose 4B resin to select for the binding of RNA fragments. Then, the selected RNA fragments were reverse transcribed to DNA using adaptor primers. PCR amplification with specific primers was used to determinate the proper number of cycles to distinguish sample and negative controls. After that, PCR products were purified and used as a template to generate the next-round RNA library by in vitro transcription. The selection was repeated six times, and the final products were gel purified, ligated into pGEM-T Easy vector (Promega), and sequenced.

ChIP Assay

ChIP experiments were performed as described (Bowler et al., 2004; Xiao et al., 2013) using 2 g of young seedling tissue for each sample. Antibodies with specificity to H3K4me2, H3K4me3, H3K27me3 (Millipore), or H3K36me3 (Signalway Antibody) were used to immunoprecipitate the chromatin. The amount of immunoprecipitated *FLC* chromatin was determined by real-time PCR on different regions of the *FLC* locus as shown in Figure 7A. Primer sequences are given in the supplemental sheet. The relative abundance as a percentage of input is shown for each position checked in different genetic backgrounds. Three biological replicates were performed. One representative result is shown in Figure 7.

RIP and RT-PCR

RIP was performed as described (Xiao et al., 2014). Briefly, 3 g of Arabidopsis seedling tissue (20 d after germination growth in LD conditions) was harvested and cross-linked by 0.5% (v/v) formaldehyde. Plant material was ground and suspended in 15 mL of Honda buffer (0.44 M Suc, 1.25% [w/v] Ficoll, 2.5% [w/v] Dextran T40, 20 mM HEPES-KOH, pH 7.4, 10 mM $MgCl_2$, 0.5% [v/v] Triton X-100, 5 mM dithiothreitol, 1 mM phenylmethylsulfonyl fluoride [PMSF], and 1× plant protease inhibitors) supplemented with 8 units mL^{-1} RNase inhibitor and filtered through two layers of Miracloth (Calbiochem). Centrifugation was at 3,000*g* for 7.5 min at 4°C. The pellet was resuspended in 500 μL of nucleus lysis buffer (50 mM Tris-HCl, pH 8, 10 mM EDTA, 1% [w/v] SDS, 1 mM PMSF, and 1× plant protease inhibitors) + 160 units mL^{-1} RNase inhibitor. Samples were sonicated and centrifuged, and the supernatant was transferred to the fresh tubes. DNA concentration was measured in the samples to ensure that nuclear protein concentrations were similar in all samples. Aliquots of 100 μL were prepared. The samples were then diluted 10-fold with ChIP dilution buffer (1.1% [v/v] Triton X-100, 1.2 mM EDTA, 16.7 mM Tris-HCl, pH 8, and 167 mM NaCl) + 350 units mL^{-1} RNase inhibitor. IP was done by adding 2 μL of GRP7 antibody (purified mouse polyclonal antibody) and 20 μL of protein A agarose/salmon sperm DNA (Upstate; 16-157) prewashed three times by binding/washing buffer (150 mM NaCl, 20 mM Tris-HCl, pH 8, 2 mM EDTA, 1% [v/v] Triton X-100, 0.1% [w/v] SDS, and 1 mM PMSF) to the solution. Preimmune mouse serum was used as a negative antibody control, *grp7-1* sample served as the antigen negative control, and *grp7-1* transformed with *pGRP7:GRP7 ($R^{49}Q$)* was also used as a negative control. After incubating on a rotator for 3 h at 4°C, beads were washed four times with 1 mL of binding/washing buffer + 40 units mL^{-1} RNase inhibitor, and the protein-RNA complex was eluted with 50 μL of RIP elution buffer (100 mM Tris-HCl, pH 8, 10 mM EDTA, and 1% [w/v] SDS) + 40 units mL^{-1} RNase inhibitor. Then, the protein was degraded by proteinase K, and RNA was extracted by acidic phenol/chloroform and precipitated by ethanol supplemented with 3 M NaAc, pH 5.2, and 5 mg mL^{-1} glycogen (Ambion). The pellet was washed with 70% (v/v) ethanol, air dried, and dissolved in RNase-free water. The RNA sample was incubated with DNase I to digest the DNA contaminant.

For identification and quantification by RT-PCR, RNA samples were polyadenylated at 37°C for 30 min with 5 units of poly(A) polymerase (Takara). Poly (A)-tailed RNA was recovered by phenol/chloroform extraction and ethanol precipitation. A 5′ adapter (GeneRacer RACE ready cDNA kit; Invitrogen) was ligated to poly(A)-tailed RNA using T4 RNA ligase (Invitrogen), and the ligation products were recovered by phenol/chloroform extraction followed by ethanol precipitation. RT was performed using GeneRacer Oligo(dT) primer (SuperScript III) with 200 units of SuperScript III reverse transcriptase (Invitrogen). The first-round PCR was carried out for 22 cycles with GeneRacer 5′/3′ primers. The PCR products were separated on a 1% (w/v) agarose gel, and DNA smear from 200 to 800 bp was recovered and diluted 20-fold to be used as template for the second-round PCR with GeneRacer nested 5′/3′ primers. The PCR products were separated on a 1% (w/v) agarose gel, and DNA smear from 150 to 800 bp was recovered and diluted 50-fold to be used as template for the detection of gene fragments with gene-specific primers. For qualification and quantification, the genomic DNA served as a positive control for PCR, and input samples (without IP) were used for equal loading.

Sequence data for genes in this article can be found in the GenBank/EMBL databases under accession numbers *AtJAC1* (At3g16470), *AtJAC2* (At3g16460), *GRP7* (At2g21660), *FLC* (At5g10140), *SOC1* (At2g45660), *FT* (At1g65480), *CO* (At5g15840), *MAF1* (At1g77080), *MAF2* (At5g65050), *MAF3* (At5g65060), *MAF4* (At5g65070), *MAF5* (At5g65080), *SPL3* (At2g33810), *SPL4* (At1g53160), and *SPL5* (At3g15270).

Supplemental Data

The following supplemental materials are available.

Supplemental Figure S1. Expression pattern of AtJAC1 and its biochemical characteristics.

Supplemental Figure S2. Identification of *atjac1* mutants and *AtJAC1-OE* plants and functional analysis of AtJAC2 in flowering.

Supplemental Figure S3. AtJAC1 does not influence transcript level of photoperiod and age pathway factors.

Supplemental Figure S4. Subcellular localization of AtJAC1 and GRP7.

Supplemental Figure S5. Identification of *atjac1-1grp7* double mutant.

Supplemental Figure S6. Analysis of AtJAC1 mRNA and protein level in *grp7-1* and GRP7-OE plants.

Supplemental Figure S7. DEX-induced nuclear distribution of GRP7.

Supplemental Figure S8. The sequence preference of GRP7 binding RNA motif.

Supplemental Figure S9. Workflow of RIP.

Supplemental Figure S10. Direct binding of GRP7 to FLC antisense premRNA.

Supplemental Figure S11. GRP7 and AtJAC1 influence histone modification around transcription start site of *FLC* locus.

Supplemental Figure S12. Diagram of generating artificial RNA fragments to compete for GRP7 binding in planta.

Supplemental Figure S13. Interaction between GRP7 and other factors involved in *COOLAIR* polyadenylation regulation.

Supplemental Figure S14. Interaction between GRP7 and RRP6L1.

Supplemental Table S1. Comparison of the carbohydrate-binding specificities of AtJAC1.

Supplemental Table S2. Sequences of GRP7 binding RNA fragments screened by SELEX.

Supplemental Table S3. Prediction of GRP7 binding motif in *FLC* gene.

Supplemental Table S4. GRP7 binding motif fragments used in transforming.

Supplemental Text S1. Plasmids, antibodies, and primers used in this study.

ACKNOWLEDGMENTS

We thank Dr. Elizabeth Dennis (Commonwealth Scientific and Industrial Research Organization) for the *flc-20* seeds; the SALK Center for the *atjac1-1*, *atjac1-2*, *SALK_028332*, *SALK_007963*, and *grp7-1* seeds; Dr. Jianru Zuo (Institute of Genetics and Development, Chinese Academy of Sciences) for providing the DEX-inducible system; and Dr. Ildoo Hwang (Pohang University of Science and Technology) and Dr. Sang-Dong Yoo (Sungkyunkwan University) for the DEX-inducible transient expression system.

Received May 26, 2015; accepted September 17, 2015; published September 21, 2015.

LITERATURE CITED

Alonso JM, Stepanova AN, Leisse TJ, Kim CJ, Chen H, Shinn P, Stevenson DK, Zimmerman J, Barajas P, Cheuk R, et al (2003) Genome-wide insertional mutagenesis of Arabidopsis thaliana. Science **301:** 653–657

Amasino R (2010) Seasonal and developmental timing of flowering. Plant J **61:** 1001–1013

Aucouturier P, Pineau N, Brugier JC, Mihaesco E, Duarte F, Skvaril F, Preud'homme JL (1989) Jacalin: a new laboratory tool in immunochemistry and cellular immunology. J Clin Lab Anal **3:** 244–251

Babosha AV (2008) Inducible lectins and plant resistance to pathogens and abiotic stress. Biochemistry (Mosc) **73:** 812–825

Bae MS, Cho EJ, Choi EY, Park OK (2003) Analysis of the Arabidopsis nuclear proteome and its response to cold stress. Plant J **36:** 652–663

Bailey TL, Boden M, Buske FA, Frith M, Grant CE, Clementi L, Ren J, Li WW, Noble WS (2009) MEME SUITE: tools for motif discovery and searching. Nucleic Acids Res **37:** W202–W208

Bastow R, Mylne JS, Lister C, Lippman Z, Martienssen RA, Dean C (2004) Vernalization requires epigenetic silencing of FLC by histone methylation. Nature **427:** 164–167

Bäurle I, Dean C (2006) The timing of developmental transitions in plants. Cell **125:** 655–664

Bowler C, Benvenuto G, Laflamme P, Molino D, Probst AV, Tariq M, Paszkowski J (2004) Chromatin techniques for plant cells. Plant J **39:** 776–789

Brown JW, Birmingham A, Griffiths PE, Jossinet F, Kachouri-Lafond R, Knight R, Lang BF, Leontis N, Steger G, Stombaugh J, et al (2009) The RNA structure alignment ontology. RNA **15:** 1623–1631

Cao S, Jiang L, Song S, Jing R, Xu G (2006) AtGRP7 is involved in the regulation of abscisic acid and stress responses in Arabidopsis. Cell Mol Biol Lett **11:** 526–535

Chong K, Bao SL, Xu T, Tan KH, Liang TB, Zeng JZ, Huang HL, Xu J, Xu ZH (1998) Functional analysis of the *ver* gene using antisense transgenic wheat. Physiol Plant **102:** 87–92

Crevillén P, Dean C (2011) Regulation of the floral repressor gene FLC: the complexity of transcription in a chromatin context. Curr Opin Plant Biol **14:** 38–44

Crevillén P, Sonmez C, Wu Z, Dean C (2013) A gene loop containing the floral repressor FLC is disrupted in the early phase of vernalization. EMBO J **32:** 140–148

Csorba T, Questa JI, Sun Q, Dean C (2014) Antisense COOLAIR mediates the coordinated switching of chromatin states at FLC during vernalization. Proc Natl Acad Sci USA **111:** 16160–16165

Deng X, Gu L, Liu C, Lu T, Lu F, Lu Z, Cui P, Pei Y, Wang B, Hu S, et al (2010) Arginine methylation mediated by the *Arabidopsis* homolog of PRMT5 is essential for proper pre-mRNA splicing. Proc Natl Acad Sci USA **107:** 19114–19119

Fornara F, de Montaigu A, Coupland G (2010) SnapShot: control of flowering in *Arabidopsis*. Cell **141:** 550–550.e2

Fu ZQ, Guo M, Jeong BR, Tian F, Elthon TE, Cerny RL, Staiger D, Alfano JR (2007) A type III effector ADP-ribosylates RNA-binding proteins and quells plant immunity. Nature **447:** 284–288

Hackmann C, Korneli C, Kutyniok M, Köster T, Wiedenlübbert M, Müller C, Staiger D (2014) Salicylic acid-dependent and -independent impact of an RNA-binding protein on plant immunity. Plant Cell Environ **37:** 696–706

He Y (2012) Chromatin regulation of flowering. Trends Plant Sci **17:** 556–562

He Y, Amasino RM (2005) Role of chromatin modification in flowering-time control. Trends Plant Sci **10:** 30–35

Helliwell CA, Robertson M, Finnegan EJ, Buzas DM, Dennis ES (2011) Vernalization-repression of Arabidopsis FLC requires promoter sequences but not antisense transcripts. PLoS One **6:** e21513

Helliwell CA, Wesley SV, Wielopolska AJ, Waterhouse PM (2002) High-throughput vectors for efficient gene silencing in plants. Funct Plant Biol **29:** 1217–1225

Hornyik C, Terzi LC, Simpson GG (2010) The spen family protein FPA controls alternative cleavage and polyadenylation of RNA. Dev Cell **18:** 203–213

Jiang JF, Han Y, Xing LJ, Xu YY, Xu ZH, Chong K (2006) Cloning and expression of a novel cDNA encoding a mannose-specific jacalin-related lectin from *Oryza sativa*. Toxicon **47:** 133–139

Jiang SY, Ma Z, Ramachandran S (2010) Evolutionary history and stress regulation of the lectin superfamily in higher plants. BMC Evol Biol **10:** 79

Kabir S (1998) Jacalin: a jackfruit (Artocarpus heterophyllus) seed-derived lectin of versatile applications in immunobiological research. J Immunol Methods **212:** 193–211

Kim JS, Jung HJ, Lee HJ, Kim KA, Goh CH, Woo Y, Oh SH, Han YS, Kang H (2008) Glycine-rich RNA-binding protein 7 affects abiotic stress responses by regulating stomata opening and closing in *Arabidopsis thaliana*. Plant J **55:** 455–466

Kim JS, Park SJ, Kwak KJ, Kim YO, Kim JY, Song J, Jang B, Jung CH, Kang H (2007) Cold shock domain proteins and glycine-rich RNA-binding proteins from *Arabidopsis thaliana* can promote the cold adaptation process in *Escherichia coli*. Nucleic Acids Res **35:** 506–516

Komath SS, Kavitha M, Swamy MJ (2006) Beyond carbohydrate binding: new directions in plant lectin research. Org Biomol Chem **4:** 973–988

Köster T, Meyer K, Weinholdt C, Smith LM, Lummer M, Speth C, Grosse I, Weigel D, Staiger D (2014) Regulation of pri-miRNA processing by the hnRNP-like protein AtGRP7 in Arabidopsis. Nucleic Acids Res **42:** 9925–9936

Lam SK, Ng TB (2011) Lectins: production and practical applications. Appl Microbiol Biotechnol **89:** 45–55

Lannoo N, Van Damme EJ (2010) Nucleocytoplasmic plant lectins. Biochim Biophys Acta **1800:** 190–201

León J, Rojo E, Titarenko E, Sánchez-Serrano JJ (1998) Jasmonic acid-dependent and -independent wound signal transduction pathways are differentially regulated by Ca^{2+}/calmodulin in *Arabidopsis thaliana*. Mol Gen Genet **258:** 412–419

Lim MH, Kim J, Kim YS, Chung KS, Seo YH, Lee I, Kim J, Hong CB, Kim HJ, Park CM (2004) A new *Arabidopsis* gene, *FLK*, encodes an RNA binding protein with K homology motifs and regulates flowering time via *FLOWERING LOCUS C*. Plant Cell **16:** 731–740

Liu F, Marquardt S, Lister C, Swiezewski S, Dean C (2010) Targeted 3′ processing of antisense transcripts triggers *Arabidopsis* FLC chromatin silencing. Science **327:** 94–97

Liu F, Quesada V, Crevillén P, Bäurle I, Swiezewski S, Dean C (2007) The *Arabidopsis* RNA-binding protein FCA requires a lysine-specific demethylase 1 homolog to downregulate FLC. Mol Cell **28:** 398–407

Liu Y, Dai SJ, Xing LJ, Xu YY, Chong K (2015) O-linked β-N-acetylglucosamine modification and its biological functions. Sci Bull **60:** 1055–1061

Lummer M, Humpert F, Steuwe C, Caesar K, Schüttpelz M, Sauer M, Staiger D (2011) Reversible photoswitchable DRONPA-s monitors nucleocytoplasmic transport of an RNA-binding protein in transgenic plants. Traffic **12:** 693–702

Mangeon A, Junqueira RM, Sachetto-Martins G (2010) Functional diversity of the plant glycine-rich proteins superfamily. Plant Signal Behav **5:** 99–104

Marquardt S, Raitskin O, Wu Z, Liu F, Sun Q, Dean C (2014) Functional consequences of splicing of the antisense transcript COOLAIR on FLC transcription. Mol Cell **54:** 156–165

Michaels SD, Amasino RM (1999) *FLOWERING LOCUS C* encodes a novel MADS domain protein that acts as a repressor of flowering. Plant Cell **11:** 949–956

Moreira RdeA, Ainouz IL, De Oliveira JT, Cavada BS (1991) Plant lectins, chemical and biological aspects. Mem Inst Oswaldo Cruz (Suppl 2) **86:** 211–218

Nagano AJ, Fukao Y, Fujiwara M, Nishimura M, Hara-Nishimura I (2008) Antagonistic jacalin-related lectins regulate the size of ER body-type β-glucosidase complexes in *Arabidopsis thaliana*. Plant Cell Physiol **49:** 969–980

Peumans WJ, Van Damme EJ (1995) Lectins as plant defense proteins. Plant Physiol **109:** 347–352

Peumans WJ, Van Damme EJ, Barre A, Rougé P (2001) Classification of plant lectins in families of structurally and evolutionary related proteins. Adv Exp Med Biol **491:** 27–54

Piippo M, Allahverdiyeva Y, Paakkarinen V, Suoranta UM, Battchikova N, Aro EM (2006) Chloroplast-mediated regulation of nuclear genes in *Arabidopsis thaliana* in the absence of light stress. Physiol Genomics **25:** 142–152

Putterill J, Robson F, Lee K, Simon R, Coupland G (1995) The CONSTANS gene of *Arabidopsis* promotes flowering and encodes a protein showing similarities to zinc finger transcription factors. Cell **80:** 847–857

Rabinovich GA, Toscano MA (2009) Turning 'sweet' on immunity: galectin-glycan interactions in immune tolerance and inflammation. Nat Rev Immunol **9:** 338–352

Romera-Branchat M, Andrés F, Coupland G (2014) Flowering responses to seasonal cues: what's new? Curr Opin Plant Biol **21:** 120–127

Ruelens P, de Maagd RA, Proost S, Theißen G, Geuten K, Kaufmann K (2013) FLOWERING LOCUS C in monocots and the tandem origin of angiosperm-specific MADS-box genes. Nat Commun **4:** 2280

Ryu H, Cho H, Kim K, Hwang I (2010) Phosphorylation dependent nucleocytoplasmic shuttling of BES1 is a key regulatory event in brassinosteroid signaling. Mol Cells **29:** 283–290

Schena M, Lloyd AM, Davis RW (1991) A steroid-inducible gene expression system for plant cells. Proc Natl Acad Sci USA **88:** 10421–10425

Schöning JC, Streitner C, Page DR, Hennig S, Uchida K, Wolf E, Furuya M, Staiger D (2007) Auto-regulation of the circadian slave oscillator component AtGRP7 and regulation of its targets is impaired by a single RNA recognition motif point mutation. Plant J **52:** 1119–1130

Sharon N (2008) Lectins: past, present and future. Biochem Soc Trans **36:** 1457–1460

Sheldon CC, Burn JE, Perez PP, Metzger J, Edwards JA, Peacock WJ, Dennis ES (1999) The *FLF MADS* box gene: a repressor of flowering in *Arabidopsis* regulated by vernalization and methylation. Plant Cell **11:** 445–458

Shin JH, Chekanova JA (2014) Arabidopsis RRP6L1 and RRP6L2 function in FLOWERING LOCUS C silencing via regulation of antisense RNA synthesis. PLoS Genet **10:** e1004612

Song J, Irwin J, Dean C (2013a) Remembering the prolonged cold of winter. Curr Biol **23:** R807–R811

Song M, Xu W, Xiang Y, Jia H, Zhang L, Ma Z (2013b) Association of jacalin-related lectins with wheat responses to stresses revealed by transcriptional profiling. Plant Mol Biol **84:** 95–110

Srikanth A, Schmid M (2011) Regulation of flowering time: all roads lead to Rome. Cell Mol Life Sci **68:** 2013–2037

Staiger D, Zecca L, Wieczorek Kirk DA, Apel K, Eckstein L (2003) The circadian clock regulated RNA-binding protein AtGRP7 autoregulates its expression by influencing alternative splicing of its own pre-mRNA. Plant J **33:** 361–371

Streitner C, Danisman S, Wehrle F, Schöning JC, Alfano JR, Staiger D (2008) The small glycine-rich RNA binding protein AtGRP7 promotes floral transition in *Arabidopsis thaliana*. Plant J **56:** 239–250

Streitner C, Köster T, Simpson CG, Shaw P, Danisman S, Brown JWS, Staiger D (2012) An hnRNP-like RNA-binding protein affects alternative splicing by in vivo interaction with transcripts in *Arabidopsis thaliana*. Nucleic Acids Res **40:** 11240–11255

Sun Q, Csorba T, Skourti-Stathaki K, Proudfoot NJ, Dean C (2013) R-loop stabilization represses antisense transcription at the Arabidopsis FLC locus. Science **340:** 619–621

Swiezewski S, Liu F, Magusin A, Dean C (2009) Cold-induced silencing by long antisense transcripts of an Arabidopsis Polycomb target. Nature **462:** 799–802

Tamaoki M, Freeman JL, Pilon-Smits EA (2008) Cooperative ethylene and jasmonic acid signaling regulates selenite resistance in Arabidopsis. Plant Physiol **146:** 1219–1230

Tang W, Deng Z, Oses-Prieto JA, Suzuki N, Zhu S, Zhang X, Burlingame AL, Wang ZY (2008) Proteomics studies of brassinosteroid signal transduction using prefractionation and two-dimensional DIGE. Mol Cell Proteomics **7:** 728–738

Thilmony R, Underwood W, He SY (2006) Genome-wide transcriptional analysis of the *Arabidopsis thaliana* interaction with the plant pathogen *Pseudomonas syringae* pv. *tomato* DC3000 and the human pathogen *Escherichia coli* O157:H7. Plant J **46:** 34–53

Tuerk C, Gold L (1990) Systematic evolution of ligands by exponential enrichment: RNA ligands to bacteriophage T4 DNA polymerase. Science **249:** 505–510

Vandenborre G, Smagghe G, Van Damme EJ (2011) Plant lectins as defense proteins against phytophagous insects. Phytochemistry **72:** 1538–1550

Wang JW, Czech B, Weigel D (2009) miR156-regulated SPL transcription factors define an endogenous flowering pathway in *Arabidopsis thaliana*. Cell **138:** 738–749

Wang ZW, Wu Z, Raitskin O, Sun Q, Dean C (2014) Antisense-mediated FLC transcriptional repression requires the P-TEFb transcription elongation factor. Proc Natl Acad Sci USA **111:** 7468–7473

Wu G, Park MY, Conway SR, Wang JW, Weigel D, Poethig RS (2009) The sequential action of miR156 and miR172 regulates developmental timing in *Arabidopsis*. Cell **138:** 750–759

Xiang Y, Song M, Wei Z, Tong J, Zhang L, Xiao L, Ma Z, Wang Y (2011) A jacalin-related lectin-like gene in wheat is a component of the plant defence system. J Exp Bot **62:** 5471–5483

Xiao J, Xu S, Li C, Xu Y, Xing L, Niu Y, Huan Q, Tang Y, Zhao C, Wagner D, et al (2014) O-GlcNAc-mediated interaction between VER2 and TaGRP2 elicits *TaVRN1* mRNA accumulation during vernalization in winter wheat. Nat Commun **5:** 4572

Xiao J, Zhang H, Xing L, Xu S, Liu H, Chong K, Xu Y (2013) Requirement of histone acetyltransferases HAM1 and HAM2 for epigenetic modification of FLC in regulating flowering in Arabidopsis. J Plant Physiol **170:** 444–451

Xing L, Li J, Xu Y, Xu Z, Chong K (2009) Phosphorylation modification of wheat lectin VER2 is associated with vernalization-induced O-GlcNAc signaling and intracellular motility. PLoS One **4:** e4854

Yang H, Howard M, Dean C (2014) Antagonistic roles for H3K36me3 and H3K27me3 in the cold-induced epigenetic switch at *Arabidopsis FLC*. Curr Biol **24:** 1793–1797

Yong WD, Xu YY, Xu WZ, Wang X, Li N, Wu JS, Liang TB, Chong K, Xu ZH, Tan KH, et al (2003) Vernalization-induced flowering in wheat is mediated by a lectin-like gene VER2. Planta **217:** 261–270

Yoo SD, Cho YH, Sheen J (2007) Arabidopsis mesophyll protoplasts: a versatile cell system for transient gene expression analysis. Nat Protoc **2:** 1565–1572